Masters Theses   Graduate School

5-2005

Cure-Induced Stress Control in Thermosetting Polymer Composites

Richard W. Burgess
University of Tennessee - Knoxville

To the Graduate Council:

I am submitting herewith a thesis written by Richard W. Burgess entitled "Cure-Induced Stress Control in Thermosetting Polymer Composites." I have examined the final electronic copy of this thesis for form and content and recommend that it be accepted in partial fulfillment of the requirements for the degree of Master of Science, with a major in Aerospace Engineering.

Madhu S. Madhukar, Major Professor

We have read this thesis and recommend its acceptance:

Kevin M. Kit, Mancil W. Milligan
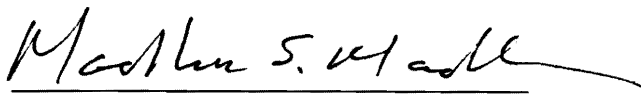
Accepted for the Council:
Dixie L. Thompson

Vice Provost and Dean of the Graduate School

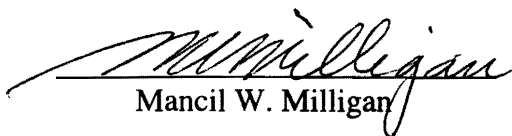(Original signatures are on file with official student records.)

To the Graduate Council:

I am submitting herewith a thesis written by Richard Wayne Burgess entitled "Cure-Induced Stress Control in Thermosetting Polymer Composites." I have examined the final paper copy of this thesis for form and content and recommend that it be accepted in partial fulfillment of the requirements for the degree of Master of Science, with a major in Aerospace Engineering.

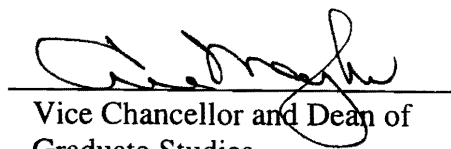Madhu S. Madhukar, Major Professor

We have read this thesis
and recommend its acceptance:

Kevin M. Kit

Mancil W. Milligan

Acceptance for the Council:

Vice Chancellor and Dean of
Graduate Studies

Cure-Induced Stress Control in Thermosetting Polymer Composites

A Thesis
Presented for the
Master of Science Degree
The University of Tennessee, Knoxville

Richard Wayne Burgess
May 2005

Acknowledgements

Abstract

During the cure of polymer matrix composites, induced stresses develop due to shrinkage of the matrix material. Consequences of this can lead to shifting of the reinforcement, adversely affecting final properties of the material, or the induced stresses can alter the final geometry of the part. With the use of a new closed loop feedback program developed, residual stresses built up during cure were minimized. Experiments were performed using the EPON 828 resin with two types of reinforcement, carbon and glass fiber. The residual stress built up during the optimized cure cycle was compared with that produced during the manufacturer recommended 2-step cure cycle and isothermal cure cycles. Results for both fibers show a large reduction in stresses endured during cure for the optimized cure compared to typical stresses seen under isothermal and standard cure cycles. Static and dynamic testing were done on specimens and showed that the modulus and the glass transition temperatures of cured specimens were not significantly affected by the optimized cure cycles. Results also show that optimized cure cycles were of shorter duration compared to the standard cure cycles.

Table of Contents

List of Tables

List of Figures

1. Introduction

Thermosetting polymer composites have found a wide variety of applications today increasingly being used in the automotive, electronics and aerospace industries to make everything from circuitry boards to aircraft structures. They are appealing because of their high strength to weight ratios and high stiffness. Also, depending on the constituents used, the composite may show excellent corrosive resistance, thermal/electrical insulation and/or fatigue performance. The major setback impeding thermosetting polymers in finding more extensive use is the expensive manufacturing costs due in part to added labor in subcomponent assembly because of lack of control of dimensional tolerance. For this reason, a large composite part is often fabricated by assembling smaller components. The rationale for manufacturing multiple subcomponents rather than one seamless part is a result of the internal stresses that develop during processing. The alleviation of these stresses occurs in the form of part warpage, fiber waviness and/or microcracking of the polymer matrix. The warping of parts results in a more labor-intensive assembly of subcomponents, requiring the use of shims to align joining parts. While fiber waviness and microcracking lead to a decline in mechanical properties, and a final part that does not meet engineers original design specifications.

It is well known that stresses develop inside a thermoset polymer composite due to the volume changes of the polymer matrix during cure. During a typical temperature-time cure cycle, a polymer undergoes both expansion as well as shrinkage in its volume.

During a heat up ramp, the polymer volume increases due to thermal expansion. In addition, the energy added to the polymer in the form of heat results in a chemical reaction inside the polymer where crosslinks are formed between molecular chains. The crosslink produces a tighter network, which causes a decrease in the polymer volume and is referred to as chemical shrinkage. For some polymers, this chemical shrinkage has been shown to progress linearly with the degree of cure of the polymer [1]. During cooldown, the volume decrease is primarily due to thermal shrinkage. These volume changes have been measured using a volumetric dilatometer during the cure of some common aerospace polymers [1-2]. As the interfacial bond between the embedded fibers and the polymer strengthens and as the polymer develops stiffness during the cure process, these volume changes strain the embedded reinforcement, which experiences essentially negligible volume change compared to the matrix. This thermal expansion mismatch between the fiber and the polymer matrix and the chemical shrinkage of polymer during cure are the root causes of residual stress.

The point of gelation (gel point) in a cure cycle refers to the polymers transition from a viscous liquid to a viscoelastic solid. It is the point in which all molecular chains in the polymer are connected through crosslinks and the polymer network can be considered to be one large molecule. Before the gel point, stress relaxation times are small as the polymer still behaves like a liquid. As the curing process approaches the gel point, stress relaxation times increase and the cure-induced stresses produced on the reinforcements cannot be relieved fast enough. The resulting stresses start to accumulate and make up a portion of the final residual stress found in the composite. One study on epoxies shows

2

that as much as 30% of the final residual stress encountered, occur during the curing process [3]. The remainder of the residual stress occurs in the cooldown phase of the cure process as the material returns to room temperature. Here, the stresses arise due to thermal shrinkage. Controlling the temperature gradient during cooldown has been shown to reduce residual stresses [4]. Techniques exist to measure the actual residual stress found in a particular part [5-7].

Experimenting with optimized cure cycles using the trial and error approach becomes costly from a materials aspect. This is why many different processing models have been developed with the intention of determining optimal cure cycles numerically by predicting residual stress buildup [8-15]. Based on the conservation principles, these approaches use numerical methods to predict potential warpage during cure. Some models account for both chemical and thermal strains that develop during the curing process, assuming linear viscoelastic behavior of the material.

Techniques have been developed to measure the residual stress during cure with strain gages or load cells and using this knowledge, develop an optimal cure cycle [16-18]. This allows for the actual stresses built up in cure for any particular specimen to be viewed. Another approach has been to use a feedback technique to optimize the cure cycle in real time with stress data being recorded [19].

It can be seen that a great deal of effort has been put forth to examine and reduce the evolution of residual stresses. In this thesis, the objective was to minimize residual stress

3

by optimizing the cure cycle using knowledge of polymer volume shrinkage/expansion to offset one another. This offset in volume change would induce little to no strain on the reinforcement and consequently result in lower residual stresses. This was done using a new closed loop feedback approach to monitor the residual stress buildup during the cure cycle and adjust the temperature during the cure process accordingly. From this, a new cure cycle was found based on the heating path that allowed the smallest increase in stress on the reinforcement. Results for the closed loop feedback approach show minimal residual stress buildup during cure in addition to shorter processing times compared to the manufacturer recommended cure cycle.

2. Materials & Experimental Procedure

2.1 Materials

The resin used for all experiments was Epon 828, manufactured by Shell Chemicals. This was used in conjunction with the curing agent metaphenylenediamine (mPDA), manufactured by Dupont Chemicals. The two types of fibers used for reinforcements were S2 glass fiber and AS4 graphite. A type K thermocouple was used for temperature measurements.

Preparation of the epoxy involved the mixture of 14 parts per 100 by weight of the curing agent to the resin. The mPDA was heated separately until molten; resin was then added and mixed in at room temperature. This was followed by a period of degassing for five minutes at 70°C (158 F) to remove entrapped air in epoxy introduced during mixing.

2.2 Setup

A single fiber is bonded to a fixed support at one end and to a load cell at the other. The fiber was given a pretension of 350 mV (0.0385 N) to ensure a straight fiber and so any increase or decrease in fiber tension could be easily observed. A platform below is raised up to the fiber where a silicon mold tray is positioned. The fiber is aligned and recessed into grooves on the mold without contacting the walls of the mold. Next the epoxy is slowly injected into the mold from one end using a syringe. This is done so the initially low viscosity epoxy will flow through the channel and distribute evenly to avoid trapping

air under/in the sample. The thermocouple is positioned in the center of the mold just above the surface of the epoxy. A ceramic block with a small channel cut out to straddle the fiber and silicone tray is placed over the specimen. Finally, a heating strip is placed over top the setup, resting on the ceramic block. Figure 1 shows a schematic diagram of the cure-induced stress test (CIST). Further details of the setup can be found in another paper [20].

Parameters controlled during the CIST are heating rates, hold times and total run time, which allow cure cycles to be tailored as desired. A multi-temperature curing cycle can also be performed. The program records the axial load on the fiber from the load cell, temperature from a thermocouple inside the chamber and the time at which they occur. Cooldown data can also be recorded to see the effects of thermal shrinkage.

Before optimizing the cure cycle for a given fiber-matrix system, two types of cure cycles were used – 1) the standard cure cycle recommended by the resin manufacturer, and 2) the isothermal cure cycle.

The standard cure cycle for EPON 828 resin was a two-step curing cycle. The cure cycle consisted of an eight-minute ramp from room temperature to 80°C (176°F) where it was held for three hours; a 1-minute ramp to 150°C (302°F) and held for one hour; followed by an uncontrolled cooldown back to room temperature.
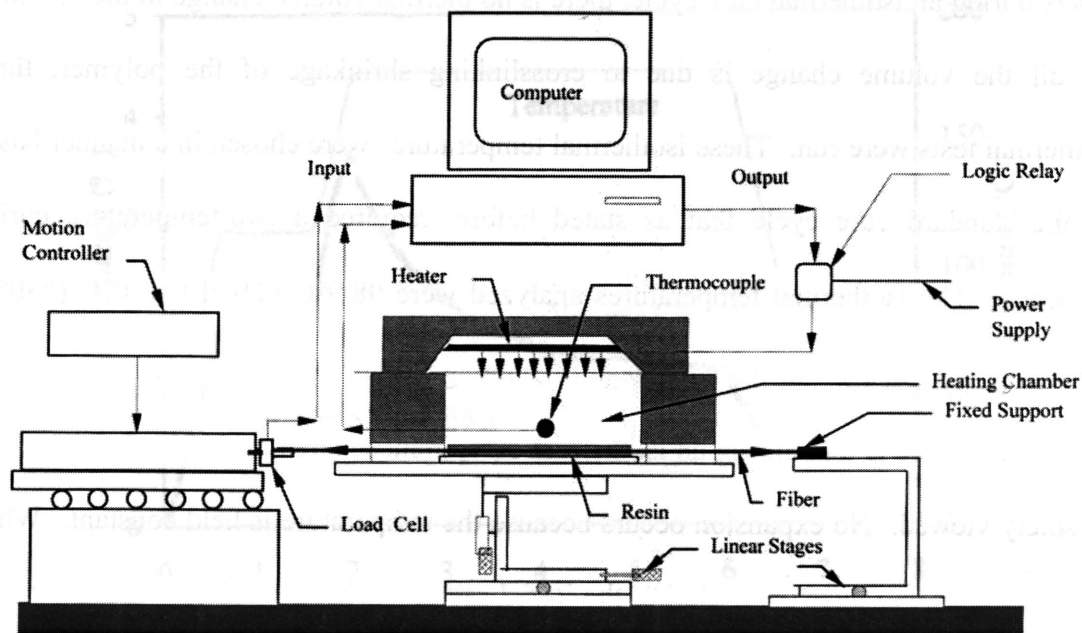
Figure 1. Schematic for the CIST setup.

Since, during an isothermal cure cycle, there is no thermal volume change in the polymer, i.e. all the volume change is due to crosslinking shrinkage of the polymer, three isothermal tests were run. These isothermal temperatures were chosen in a manner based on the standard cure cycle that as stated before, required a two-temperature curing sequence. The isothermal temperatures analyzed were 98.9°C (210°F), 110°C (230°F) and 121.1°C (250°F). So the advantage of running isothermal cure cycles compared to the standard cure is that during an isothermal cure, induced stresses due to shrinkage can be solely viewed. No expansion occurs because the temperature is held constant. While thermal expansion does occur during the initial ramp, the isothermal curing temperature is reached before the polymer reaches its gel point. Therefore no significant stresses are induced because of this thermal expansion. The CIST plots during an isothermal cure will thus provide a clear picture on the crosslinking shrinkage behavior of the polymer.

Figure 2 shows the basic trends of polymer volume change during a typical two-step cure cycle specified by the manufacturer. It can be seen that the polymer volume increases almost linearly with temperature until the first temperature dwell. This volume increase is attributed to the polymer thermal expansion. Towards the end of the first temperature dwell, there is a slight decrease in polymer volume. The decrease in polymer volume is indicative of the start of crosslinking reactions. Then during the second temperature ramp, there is a significant polymer volume increase with temperature. During this period, polymer is experiencing both expansion (thermal expansion) and shrinkage (crosslinking shrinkage). However, since there is a net increase in polymer volume, the thermal expansion dominates the crosslinking shrinkage.

8
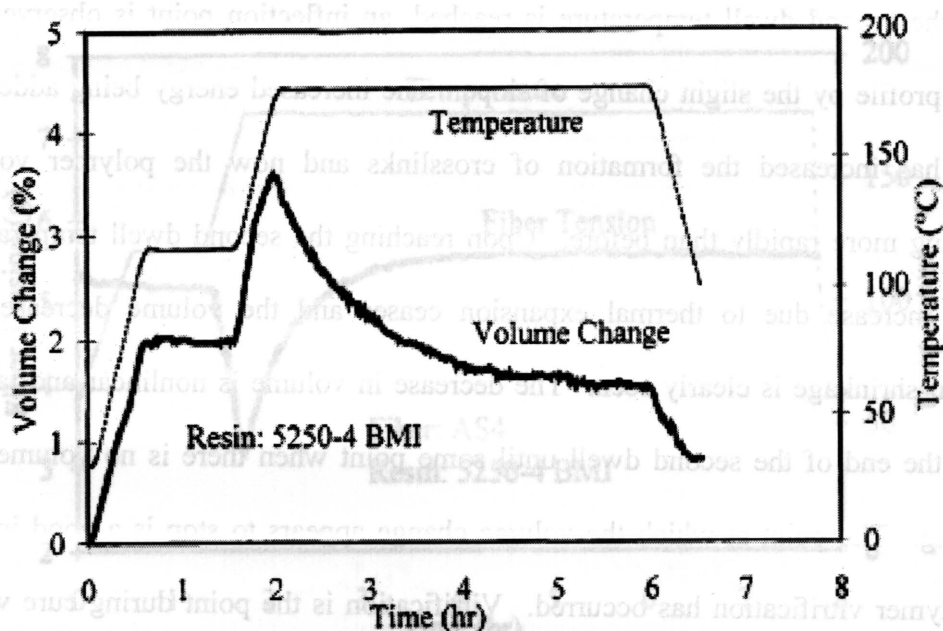
Figure 2. Volume change data of 5250-4 BMI resin during the standard cure cycle [21]. The figure shows thermal expansion during the two temperature ramps and chemical shrinkage during the second temperature hold followed by thermal shrinkage during cooldown.

Before the second dwell temperature is reached, an inflection point is observed in the volume profile by the slight change of slope. The increased energy being added to the system has increased the formation of crosslinks and now the polymer volume is decreasing more rapidly than before. Upon reaching the second dwell temperature the volume increase due to thermal expansion ceases and the volume decrease due to chemical shrinkage is clearly seen. The decrease in volume is nonlinear and tapers off toward the end of the second dwell until some point when there is no volume change occurring. The point at which the volume change appears to stop is a good indication that polymer vitrification has occurred. Vitrification is the point during cure when the bulk of the chemical reaction stops and any further reaction is diffusion controlled; when the glass transition temperature is equal to that of the curing temperature. This process can be undone with the addition of heat. Upon completion of the cure cycle, the volume decreases again due to thermal shrinkage as the temperature cools to ambient.

Figure 3 shows the corresponding change in fiber tension for the same polymer during the same cure cycle. Here, a single carbon fiber is used to measure the resulting stress during the manufacturer recommended cure cycle. The fiber tension remains constant through the initial ramp and most of the first dwell temperature. By the end of the first dwell, the polymer has started to develop some stiffness because the volume changes from this point on result in a change in the fiber tension. A decrease in fiber tension is clearly seen after the second ramp begins due to the increase in polymer volume from thermal expansion. As the second dwell temperature nears, the fiber tension is seen to
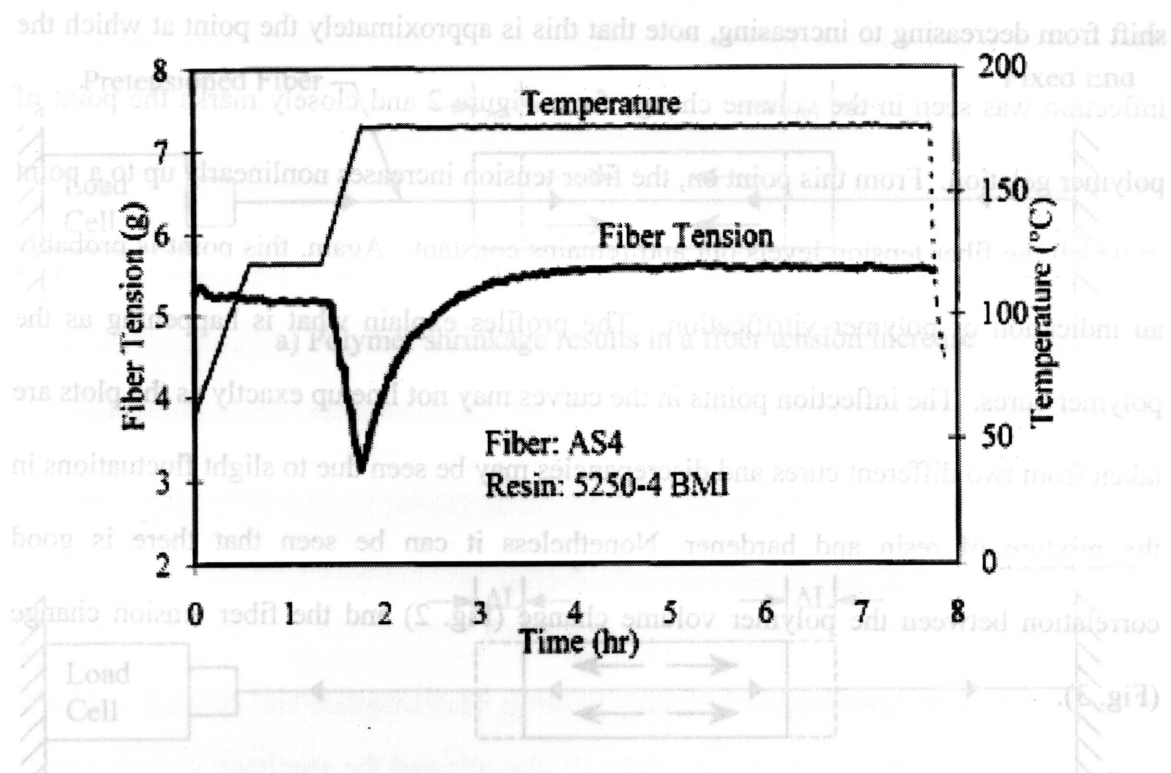
Figure 3. Fiber tension variation during the standard cure cycle of 5250-4 BMI [21]. During the second ramp the fiber tension decreases with polymer expansion and then during the second dwell temperature the fiber tension increases due to polymer shrinkage. No change in fiber tension occurs toward the end of cure.

shift from decreasing to increasing, note that this is approximately the point at which the inflection was seen in the volume change from Figure 2 and closely marks the point of polymer gelation. From this point on, the fiber tension increases nonlinearly up to a point in which the fiber tension levels out and remains constant. Again, this point is probably an indication of polymer vitrification. The profiles explain what is happening as the polymer cures. The inflection points in the curves may not line up exactly as the plots are taken from two different cures and discrepancies may be seen due to slight fluctuations in the mixture of resin and hardener. Nonetheless it can be seen that there is good correlation between the polymer volume change (Fig. 2) and the fiber tension change (Fig. 3).

Note here that the fiber tension increase rather than decrease due to volumetric shrinkage is counterintuitive. The reason for this is due to shrinkage of the polymer producing compressive stresses (forces) only on the portion of the fiber passing through the polymer. However, in the CIST setup the actual length of the carbon fiber is greater than that which is in contact with the polymer. The shrinkage acts to effectively make the total fiber length shorter which is consequently registered as an increase in fiber tension to the load cell. Just the way thermal expansion induces tensile stresses (forces) on the fiber but shows up on the CIST results as a decrease in fiber tension. Figure 4 shows the schematic of these phenomena.

12
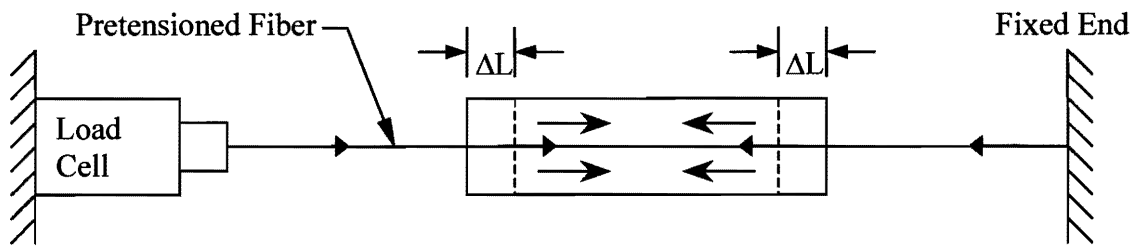
a) Polymer shrinkage results in a fiber tension increase
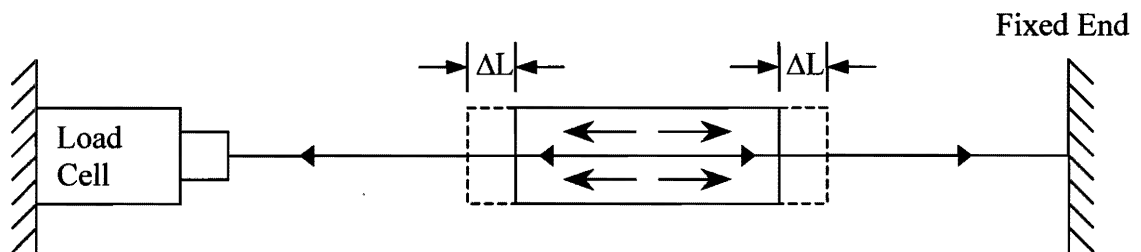
b) Polymer expansion results in a fiber tension decrease

Figure 4. Schematics of polymer shrinkage and polymer expansion and the resulting affect on fiber tension. Arrows indicate direction of displacement of fiber and polymer.

2.3 Closed Loop Feedback System (CLFS)

Cure induced stresses arise during cure due to volume changes in the polymer because of crosslinking and thermal expansion/shrinkage. A closed loop feedback (CLFS) program was developed to modify the cure cycle to minimize these stresses. The approach used in this program is to counter the cure shrinkage, which is an inevitable part of the cure cycle. This program requires inputs of initial cure temperature, ramp time, upper and lower bounds, and total curing time. The initial temperature is the temperature at which the curing process begins for the specimen. The ramp time is the time it takes to increase from room temperature to the desired initial temperature; this is nothing more than the heating rate. This time was fixed to eight minutes for all experiments since this was the ramp time used for the standard cure cycle. It also allowed the specimen enough time to gradually reach its initial curing temperature to maintain a uniform heat distribution and eventually provoke uniform crosslinking. Once the ramp is complete, the computer records the current load on the fiber from the load cell and uses this as the reference load. This reference load (or stress) is due only to the preset fiber tension as no significant residual stresses have yet built up in the specimen because the polymer is essentially still a liquid. Load boundaries are specified before the program is started and are based on the reference load. Their function is to provide a limit in the amount of change, which can occur in the fiber tension before it is considered to be cure induced as opposed to being erroneously produced. If anytime during cure the fiber tension increases above the reference load by a specified parameter (upper bound); indicating induced stresses from cure shrinkage of the polymer; the program enters a loop where the heater is turned on, forcing thermal expansion of the polymer until the tension (stress) on the fiber is

14

equivalent to that produced only by the reference load. The temperature at this moment when no cure stresses are present is maintained until the next loop is entered. A similar process occurs if the fiber tension falls below the reference load by a specified parameter (lower bound); indicating an increase in stress due to thermal expansion; except in this loop of the program the heater is shut off until the stress on the fiber is again that corresponding to the reference load. At this point the heater turns back on and provides enough heat to maintain the current temperature. This process continues until the given cure time is reached. A flow chart of this program is shown in Figure 5. A cure time of 240 minutes was used for some of the optimized experiments because this was the cure duration used for the standard cure cycle. Optimized cures using the CLFS were also performed for cure times of 180 minutes and 200 minutes for comparison.

2.4 Three-Point Bend Testing

Three point bend tests were carried out manually using a table mount, weights and uniaxial pattern strain gages at room temperature. The same progression of weight increase was used for all specimens. The strain gages had a resistance of 350 ohms with a gage factor of two and were used in conjunction with a Strain Gage Conditioning Amplifier (2310). A Fluke 21 series digital multimeter was used to read results. The average dimensions of the specimens were 7.25mm in width, 2.25mm in height and 38.1mm in length.
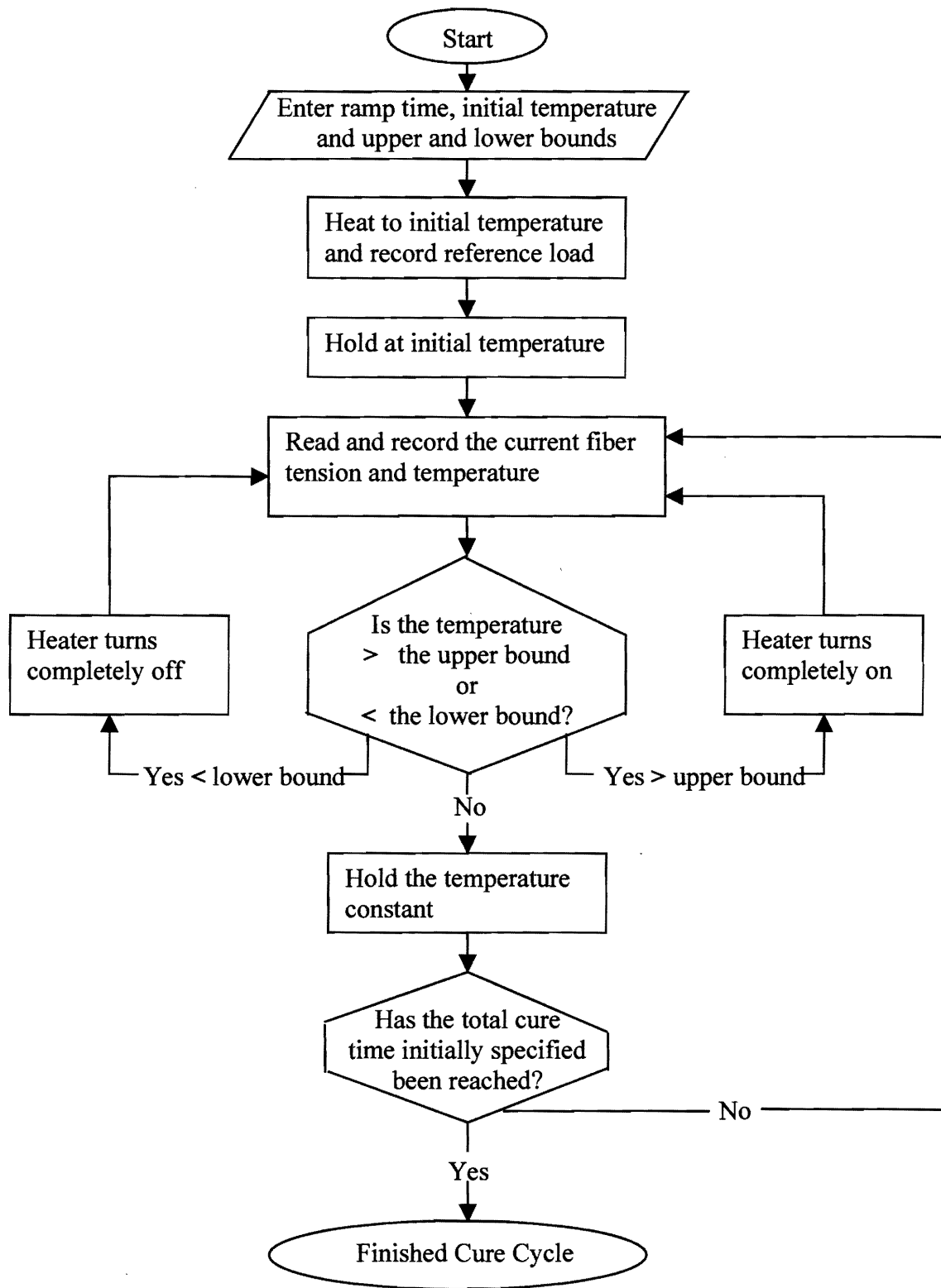
Figure 5. Flow chart of the CLFS program

2.5 Dynamic Testing

Specimens underwent dynamic testing using dynamic mechanical analysis on a Rheometric Scientific DMTA V with the 3-point bend setup. A temperature scan was performed, and the specimens were tested over the temperature range of 80 to 220°C with a heating rate of 2°C/min. A fixed frequency of 1.0Hz and a 0.1% strain were used. Specimen dimensions were roughly 3.25mm in width, 2.5mm in height and 40mm in length. The width and height varied by approximately ±10% from specimen to specimen to due preparation.

3. Results & Discussion

3.1 Glass Fiber Expansion

It is important to note that the glass fiber exhibits thermal expansion/contraction during cure while the carbon fiber does not. So the data from the isothermal cures with carbon fiber are complete after cure and can be used to observe and describe the induced stresses. The glass fiber results are not finished after cure because the fiber tension profiles do not show the absolute change in tension due to shrinkage/expansion of the polymer matrix; instead it is skewed by expansion of the glass fiber. This issue was dealt with in the results by putting the glass fiber through the same isothermal and standard cure with no epoxy and recording its change in fiber tension for the same cure time; then subtracting this data from the glass fiber and epoxy specimen cured to see only the fiber tension change due to polymer shrinkage/expansion. Figure 6 shows the three fiber tension profiles for a CIST test on glass fiber. All remaining results for glass fiber have been modified in this manner to show tension changes due only to volume changes of the polymer unless specified otherwise.

As can be seen from the "No Fiber Expansion" curve in Figure 6, which corresponds to the change in fiber tension due to polymer volume changes only, polymer shrinkage produced a gradual increase in the fiber tension during the temperature hold and then plateaus until the end of temperature hold when it increases again due to thermal shrinkage of the polymer. The purpose of this research was to address only the stresses

Isothermal Cure at 98.9°C (110°F) with Glass Fiber

Figure 6. Fiber tension profiles for glass fiber using data retrieved from CIST (With Fiber Expansion) and the corrected profile for the fiber tension having removed the expansion of the glass fiber (No Fiber Expansion) during an isothermal cure. The change in fiber tension for the glass fiber alone can also be seen.

developed during the cure and therefore any stresses developed in cooldown will not be discussed. Also note the small difference between the "Glass Fiber Alone" and "With Fiber Expansion" profiles seen at the beginning of cure. This may be due to slight variance in the fiber length or error from thermocouple placement from experiment to experiment. This deviation is translated to the "No Fiber Expansion" profile, which should remain constant along the reference line until the initial increase in fiber tension for a fiber that does not exhibit thermal expansion/contraction.

3.2 Standard Cure Cycle

Figure 7 shows the change in fiber tension for both S2 glass and AS4 graphite fiber/Epon using the manufacturer recommended cure cycle (standard cure). A more dramatic change in fiber tension is seen for the glass fiber throughout the entire cure cycle. While some of difference between the two curves may be the result of different interfacial bond strengths between the two fibers and Epon 828, it is believed that majority of the difference in fiber tension is due to the large difference in surface area of the two fibers. The diameter of the carbon fiber is about 8-13 microns while the glass fiber is about 100-130 microns. The cure behavior appears to be unaffected by either fiber choice. This is indicated by the initial increase in fiber tension occurring at approximately 80 minutes for both specimens. Towards the end of the first temperature dwell, no change in load is observed for either fiber, a possible indication of vitrification. When the temperature increases from 80°C to 150°C, the resulting thermal expansion changes the stress on the fiber from compression to tension. This is observed in Figure 7 by the fiber tension

Figure 7. Fiber tension profiles for glass and carbon fibers during the standard cure cycle of Epon/mPDA. Both fibers show similar trends in tension transitions with the glass fiber experiencing more significant changes in tension.

decreasing below that of the preset reference value. This would indicate that a strong physical bond is present between the two constituents at this stage of the cure.

Immediately following ramping to the second dwell temperature, a large increase in fiber tension occurs implying that vitrification has been undone, if indeed it had occurred earlier. This shrinkage begins to taper off at the end of cure. When the cure cycle is complete, the fiber tension increases dramatically due to thermal shrinkage. A short ramp time was used between the first and second dwell temperatures so the effects of thermal expansion could be clearly observed in the fiber tension diagrams and not be significantly offset by shrinkage. Looking at Figure 7, it is clear that some thermal expansion is being masked by shrinkage during this one-minute ramp time because immediately after the temperature becomes steady at 150°C, the fiber tension increases. It is to be noted that had a more gradual ramp occurred here, the change in fiber tension would not have been as severe because of the offsetting polymer shrinkage, but still would have fallen well below the original reference load. This is because the total fiber tension decrease due to thermal expansion during the second ramp is greater than the total fiber tension increase seen during the second temperature dwell from polymer shrinkage.

3.3 Isothermal Cures

Figure 8 shows an isothermal cure cycle for 98.9°C (210°F). Again the preset load for both fibers was approximately 0.0385 N (350mV) indicated by the dashed line. The gel point was reached around 35 minutes after curing began, shown by the first signs of fiber

CIST For Isothermal Cure at 98.9°C (210°F)
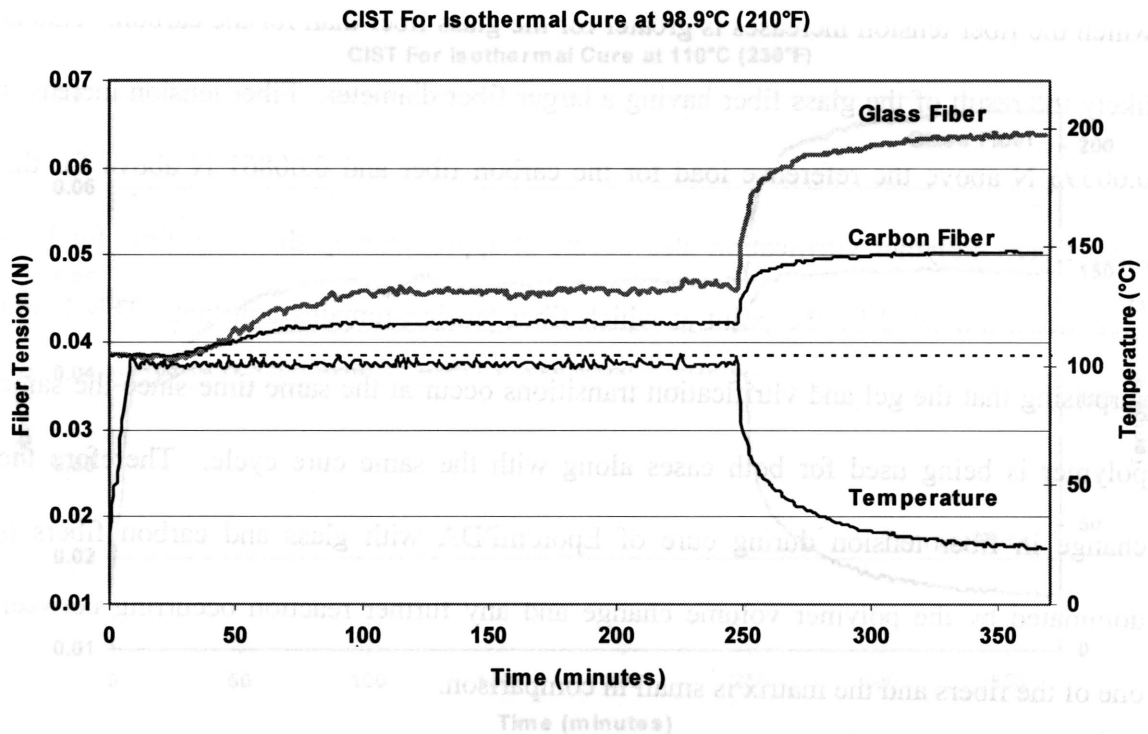
Figure 8. Fiber tension profiles during isothermal cure at 98.9°C. Tension increases for both fibers at nearly the same time but the carbon fiber profile plateaus shortly before the glass fiber.

tension increase. This happens at roughly the same time for both specimens. The rate at which the fiber tension increases is greater for the glass fiber than for the carbon. This is likely the result of the glass fiber having a larger fiber diameter. Fiber tension increases 0.00393 N above the reference load for the carbon fiber and 0.00861 N above for the glass fiber. Polymer vitrification also occurs at approximately the same time for both specimens, indicated by the point at which fiber tension remains constant. This is not surprising that the gel and vitrification transitions occur at the same time since the same polymer is being used for both cases along with the same cure cycle. Therefore the change in fiber tension during cure of Epon/mPDA with glass and carbon fibers is dominated by the polymer volume change and any further reaction occurring between one of the fibers and the matrix is small in comparison.

Figure 9 shows the CIST for both fibers at 110°C (230°F). The basic trends are similar to the previous isothermal tests. The gel point is reached much sooner for the higher temperature isothermal cure. This is expected because more energy is available for the polymer to form crosslinks, and consequently, less time is needed to reach the point where the polymer is comprised of a single polymer network. It is interesting to note here that an increase in the magnitude of fiber tension occurs for both fibers at the 110°C cure compared to the previous isothermal cure at 98.9°C. The carbon fiber increases 0.00661 N from the reference load and the glass fiber shows a 0.01209 N increase. This increase for both fibers must be due to the additional energy being added to the system resulting in an increased rate of crosslink formation. The higher rate of formation of
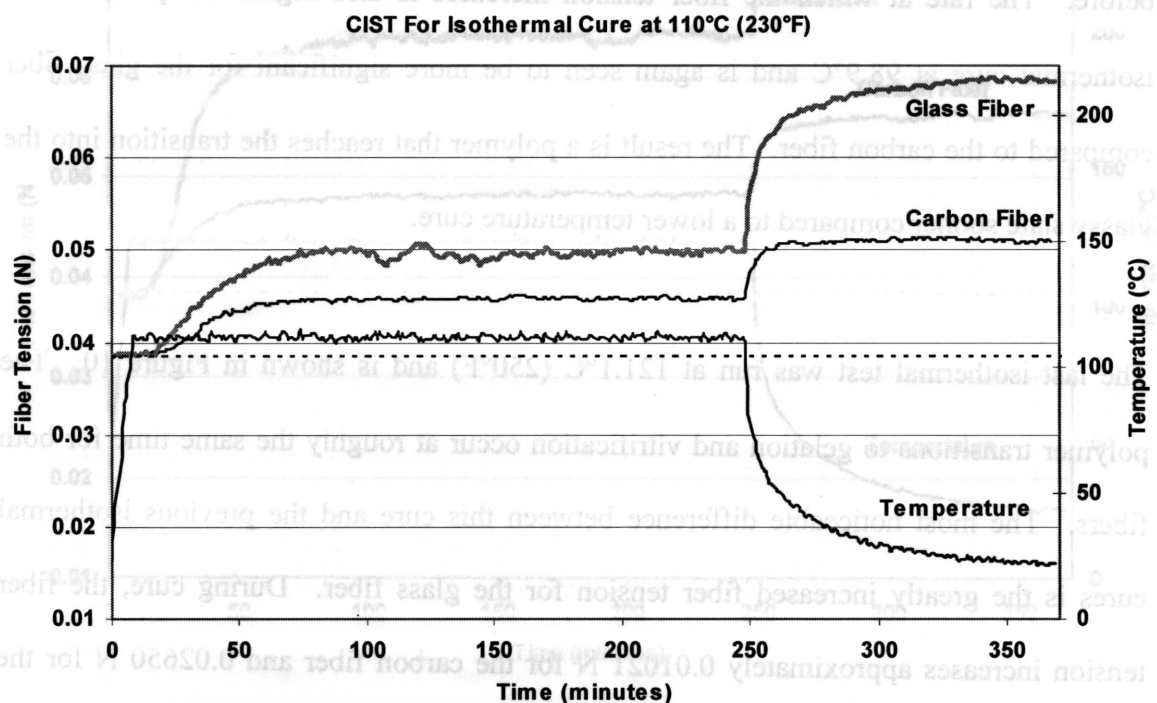
Figure 9. Fiber tension profiles during isothermal cure at 110°C. Initial tension increase occurs at similar times for both fibers and so does the plateau.

Isothermal Cure Temperature (°C)	Change in Carbon (N)	Change in Glass (N)
98.9	0.00393	0.00861
110	0.00661	0.01209
121.1	0.01021	0.02650

crosslinks acts to increase relaxation times and fiber tension change is greater than before. The rate at which the fiber tension increases is also higher compared to the isothermal cure at 98.9°C and is again seen to be more significant for the glass fiber compared to the carbon fiber. The result is a polymer that reaches the transition into the glassy state sooner compared to a lower temperature cure.

The last isothermal test was run at 121.1°C (250°F) and is shown in Figure 10. The polymer transitions to gelation and vitrification occur at roughly the same time for both fibers. The most noticeable difference between this cure and the previous isothermal cures is the greatly increased fiber tension for the glass fiber. During cure, the fiber tension increases approximately 0.01021 N for the carbon fiber and 0.02650 N for the glass fiber from the reference load. The results for the change in fiber tension for all isothermal cures are shown in Table 1. The fiber tension increase for the glass fiber is more than double that found using the isothermal cure at 110°C. The rate at which the fiber tension increases is also greater compared to the lower temperature cures. Again this higher temperature cure results in shorter amount of time in which the fiber tension is increasing, that is the time at which the fiber tension remains constant is reached sooner. This aggressive curing can lead to a material with a less developed network, as the molecular chains cannot diffuse to areas to form crosslinks [22].

The CIST cure cycles show how the residual stress grows inside the specimen during cure. It gives insight to how the chemical shrinkage, due to the crosslinking of molecular

CIST for Isothermal Cure at 121°C (250°F)
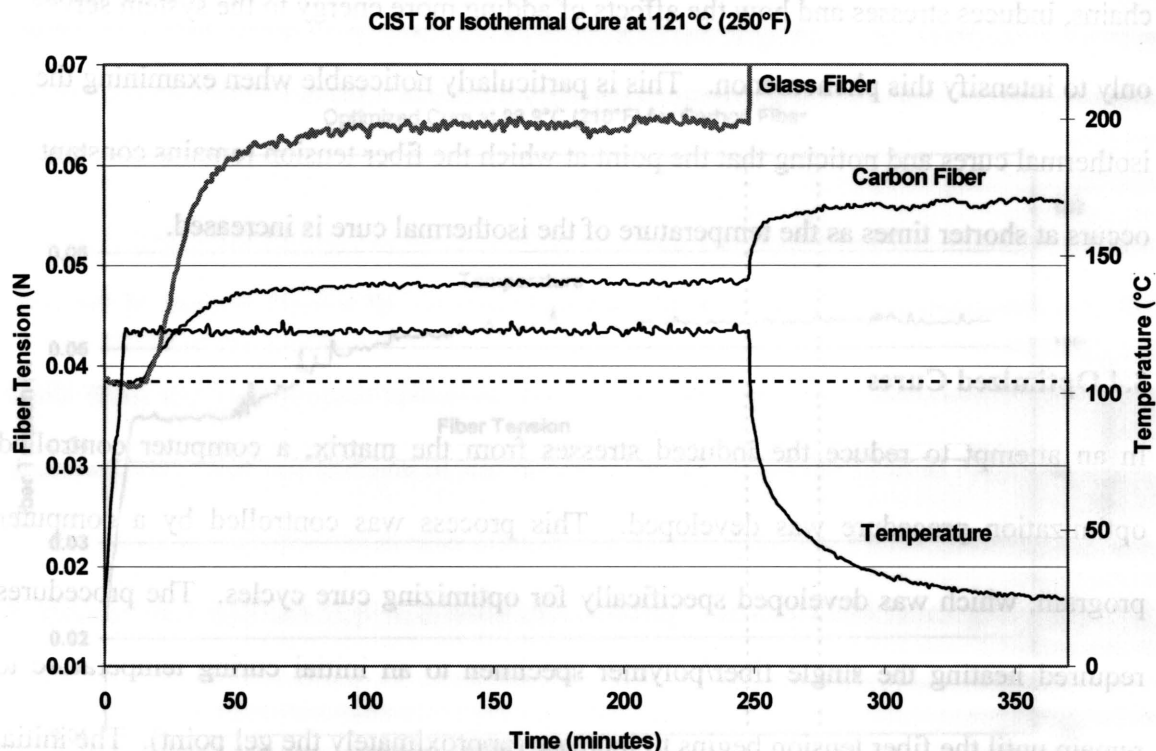
Figure 10. Fiber tension profiles during isothermal cure at 121.1°C. Initial increase and plateau of fiber tension occurs at similar times for both fibers with the glass fiber experiencing much larger increases in tension.

Table 1. Results for the maximum change in fiber tension found during cure of Epon/mPDA with carbon and Epon/mPDA with glass fiber.

Isothermal Cure Temperature (°C)	Change in Carbon Fiber Tension (N)	Change in Glass Fiber Tension (N)
98.9	0.00393	0.00861
110	0.00661	0.01209
121.1	0.01021	0.02650

chains, induces stresses and how the affects of adding more energy to the system serves only to intensify this phenomenon. This is particularly noticeable when examining the isothermal cures and noticing that the point at which the fiber tension remains constant occurs at shorter times as the temperature of the isothermal cure is increased.

3.4 Optimized Cures

In an attempt to reduce the induced stresses from the matrix, a computer controlled optimization procedure was developed. This process was controlled by a computer program, which was developed specifically for optimizing cure cycles. The procedures required heating the single fiber/polymer specimen to an initial curing temperature to remain until the fiber tension begins to increase (approximately the gel point). The initial temperatures chosen here were again 98.9°C and 110°C to compare with previous results. The basic idea here was to alleviate induced stresses from shrinkage by heating the polymer and producing just enough thermal expansion to offset the shrinkage found to occur during the isothermal tests. This addition of heat would obviously cause the temperature to increase and the cure process would reach the higher temperatures seen during postcure like in the standard cure. This would give the specimen the benefit of being cured initially at a lower temperature to flow around the reinforcement and remove and voids before increasing to higher temperatures. The overall goal here was to get a constant load on the fiber throughout the entire duration of the cure.

Figure 11 shows the optimized cure using carbon fiber for an initial temperature of

Optimized Cure at 98.9°C (210°F) for Carbon Fiber

Figure 11. Optimized cure for carbon fiber and Epon/mPDA with an initial cure temperature at 98.9°C. Fiber tension varies $\pm\,0.00033\,\mathrm{N}$. The small spikes in the temperature profile correspond to the fiber tension attempting to increase/decrease outside the specified bounds of the CLFS.
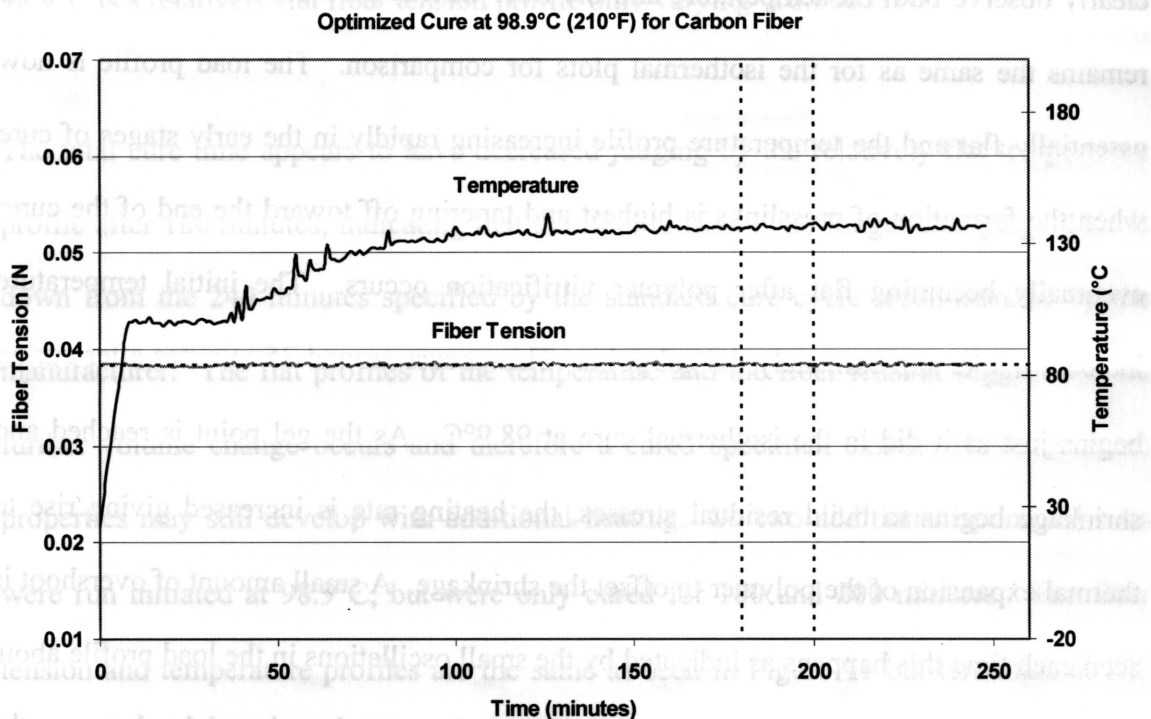
98.9°C (210°F). The temperature scale has been shifted down in the CLFS plots to clearly observe both the temperature and the fiber tension profiles, although the scaling remains the same as for the isothermal plots for comparison. The load profile is now essentially flat and the temperature profile increasing rapidly in the early stages of cure when the formation of crosslinks is highest and tapering off toward the end of the cure; eventually becoming flat after polymer vitrification occurs. The initial temperature increase marks approximately the gel point. This occurs around 35 minutes after curing begins just as it did in the isothermal cure at 98.9°C. As the gel point is reached and shrinkage begins to build residual stresses, the heating rate is increased giving rise to thermal expansion of the polymer to offset the shrinkage. A small amount of overshoot is seen each time this happens as indicated by the small oscillations in the load profile about the reference load (horizontal dashed line). This is because there is a delay between the heating or cooling and the reaction of the polymer. A finite amount of time is required for the polymer to respond to changes in energy being supplied. Therefore, each time the reference load is reached as a result of forced thermal expansion (heating) or allowed shrinkage (cooling), the momentum of the polymer volume change carries the fiber tension slightly past the reference load. The result is a load profile that oscillates slightly about the chosen reference load. The spikes witnessed in the temperature profile are further proof of this. The spikes and oscillations appear to damp out over the duration of the cure, this is probably due to the polymer passing into the glassy state (vitrification), where any further reaction is restrained by the diffusion limitations of the molecular chains. Regardless of these spikes, the optimized temperature path is clearly observed in

30

Figure 11. The result of the optimized cure cycle for carbon fiber using the CLFS at 98.9°C is a relatively flat fiber tension profile only varying ± 0.00033 N.

The total cure time appears to have decreased judging by the relatively flat temperature profile after 180 minutes, indicating that the fiber tension is no longer changing. This is down from the 240 minutes specified by the standard cure cycle recommended by the manufacturer. The flat profiles of the temperature and the fiber tension suggest that no further volume change occurs and therefore a cured specimen exists. However some properties may still develop with additional heating. So two additional optimized tests were run initiated at 98.9°C, but were only cured for 180 and 200 minutes. The fiber tension and temperature profiles are the same as seen in Figure 11 but terminate at 180 and 200 minutes, indicated by the two vertical dashed lines.

Figure 12 shows the optimized cure at 110°C (230°F) with carbon fiber. The two profiles are relatively similar to those from the CLFS done at 98.9°C. However, the magnitude of the temperature profile for the 110°C cure is larger than for the 98.9°C cure. This was expected since the magnitude of the fiber tension was seen to increase in the CIST cures from 98.9°C to 110°C. Also note the larger heating rate that is required shortly after the gel point is reached to maintain the same fiber tension compared to before. The heating rate for the CLFS at 98.9°C was about 0.7°C/min but here a heating rate of 2.3°C/min in needed. Again, part of the reason for this increased heating rate may be a result of the
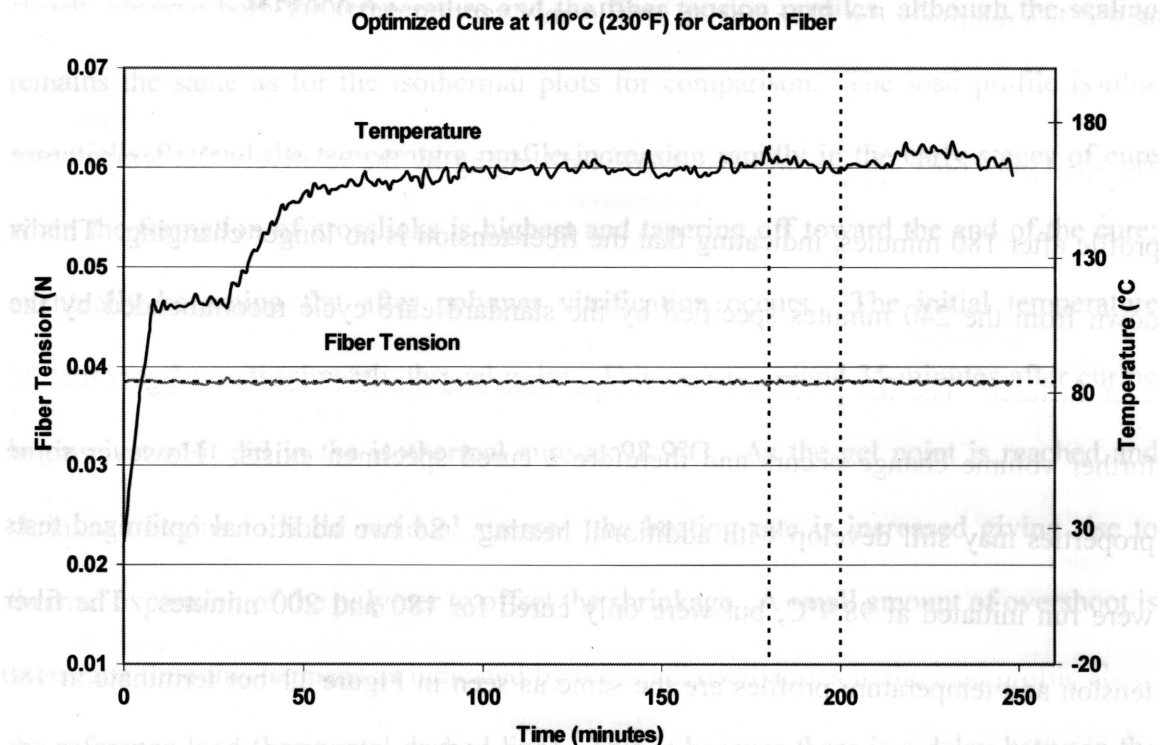
Optimized Cure at 110°C (230°F) for Carbon Fiber

Figure 12. Optimized cure for carbon fiber and Epon/mPDA with an initial cure
temperature at 110°C. Fiber tension varied ± 0.00037 N.

increased energy being supplied to the polymer increasing the formation of crosslinks and consequently increasing the shrinkage. However, increasing the shrinkage results in an increase in fiber tension, which triggers an increase in the thermal energy to offset the shrinkage. The result is a rapid cure cycle with minimized residual stresses. The optimized cure cycle for carbon fiber using the CLFS at 110°C is again, a relatively flat fiber tension profile only varying ±0.00037 N. As before, two additional optimized cures were performed with cure times of 180 and 200 minutes. The fiber tension and temperature profiles are similar to those in Figure 12, but terminating at the vertical dashed line corresponding to the decreased cure times of 180 or 200 minutes.

There does appear to be a limit to how quickly a specimen can be cured. Figure 13 shows an optimized cure with Epon/mPDA and carbon fiber using the CLFS program with an initial temperature of 121.1°C (250°F). The result was a flat fiber tension profile varying ±0.00103 N about the reference load, indicating minimal buildup of residual stress during cure, but the specimen was charred. The temperature profile can be seen to increase dramatically after the gel point to offset the polymer shrinkage. This trend of increased heating rate after the gel point was seen in the optimized cures as initial curing temperature increased (Figs. 11-13). So this shows that an upper curing limit exists for the duration of cure time using the CLFS based on the initial temperature of the cure. Similarly, if too low an initial temperature were specified, the max temperature reached during cure would not be sufficient to obtain a fully cured specimen. For all optimized cure cycles, the upper and lower bounds were specified as ±3 mV, which corresponds to ±0.00033 N.
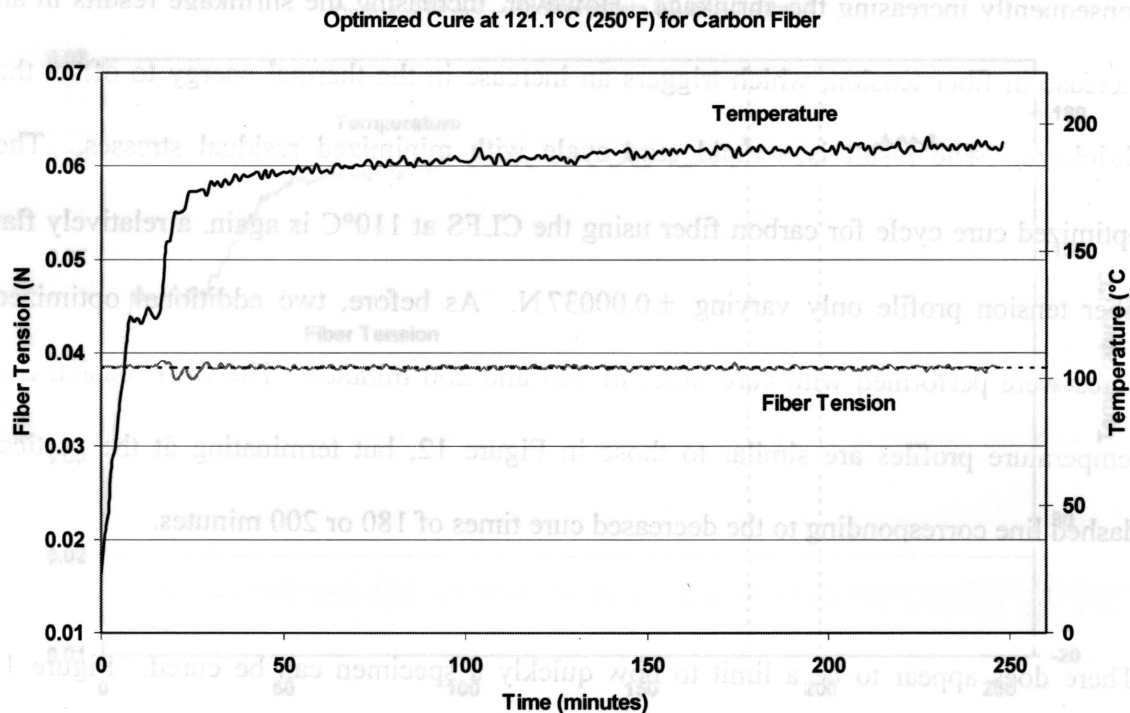
Figure 13. Optimized cure for carbon fiber and Epon/mPDA with an initial cure temperature at 121.1°C. Fiber tension varied ± 0.00103 N.

Figure 14 shows the optimized cure profiles for the glass fiber at 98.9°C (210°F). The fiber tension profile shows an initial decrease in tension due to thermal expansion of the glass fiber. Unlike with the carbon fiber where the reference load was simply the pretension on the fiber, the reference load for glass fiber was recorded after the initial drop in fiber tension had occurred. This was done so the fiber tension would not fall below the lower bound and trigger the heater to turn off in an attempt to offset the decrease in fiber tension with thermal shrinkage of the polymer. This is important because at this stage the polymer is still a fluid and no significant residual stresses have developed, indicated by the constant temperature profile. Once residual stresses do begin to develop between the two constituents, the temperature is seen to increase as before to offset the polymer shrinkage with expansion. The result of the optimized cure with glass fiber is a fiber tension profile fluctuating around the reference load ±0.00098 N, not as flat as the carbon fiber but still significantly less stress than that seen to develop during the isothermal cures.

The maximum temperature reached during the optimized cure starting at 98.9°C with glass fiber was 123°C and the max temperature reached with carbon fiber was 137°C. However, this is not the optimized cure for glass fiber because the fiber tension should in reality be seen to decrease whenever the temperature increases, since that would be the fiber tension profile if it were cured with no polymer. The goal of the CLFS is to cure the polymer around the fiber without disturbing the fiber. What is happening is the thermal
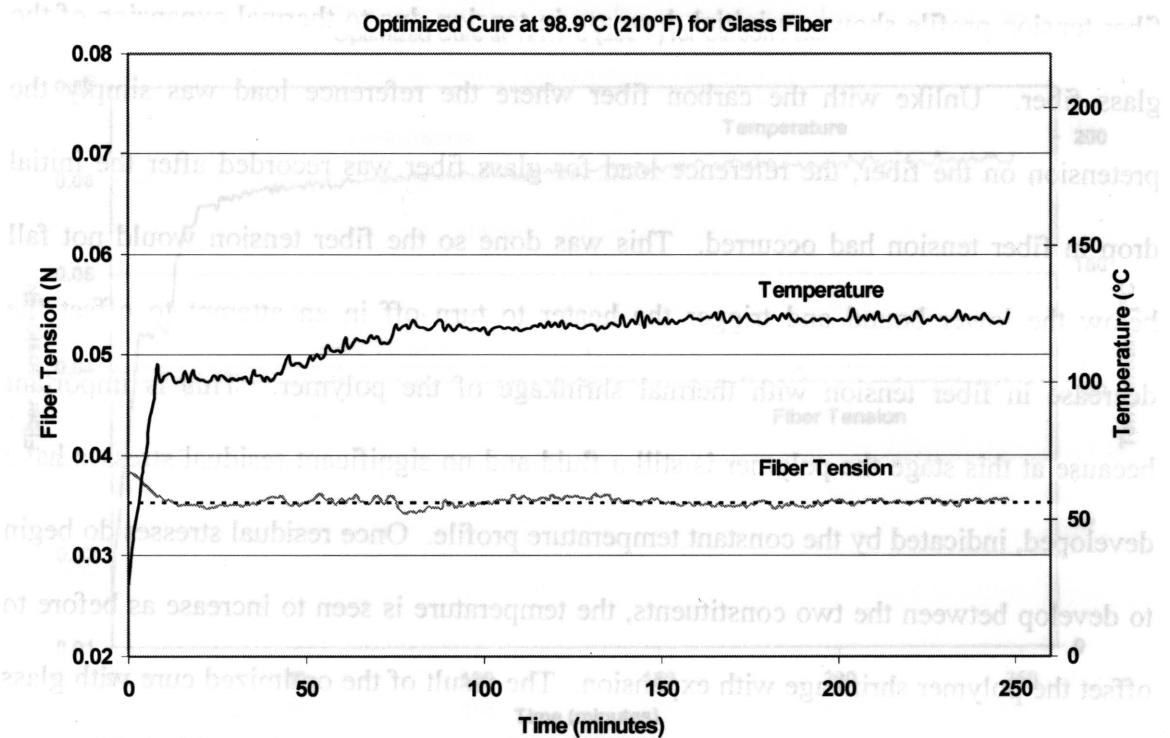
Figure 14. Optimized cure for glass fiber and Epon/mPDA with initial cure temperature at 98.9°C. The fiber tension of the glass fiber varied ± 0.00098 N.

expansion of the glass fiber is interfering with the optimized cycle. The optimized cure cycle uses thermal expansion of the polymer to offset shrinkage. In the case of the glass fiber, when the heater is turned on, the additional heat acts in part, to offset the polymer shrinkage with thermal expansion as designed, but it also makes the glass fiber length increase which acts to decrease fiber tension as well. Consequently, less heat is required to offset polymer shrinkage.

The optimized cure for the glass fiber using the CLFS approach still shows improved residual stresses compared to the standard and isothermal cures. However, it is clear that these specimens are inferior to those found using the standard cure because the temperature throughout the cure cycle never increases enough to come close to the post cure temperature of 150°C, and therefore insufficient energy is being supplied to the polymer to obtain a fully cured specimen. This is justified in Section 3.5 where the T_g is found to increase with increased curing temperature and also since the degree of cure increases with increasing T_g. Therefore, in the range of temperature tested here, the higher the temperature used during cure yielded specimens with a higher degree of cure.

For the CLFS to account for fiber expansion, a moving reference load needs to be implemented into the program. This can be done if the change in fiber tension for a particular fiber is known as function of temperature. The optimized cure for glass fiber would result in a fiber tension profile similar to that of the same temperature cure with a glass fiber and no epoxy. This would mean the polymer cured around the fiber without disturbing it. Since the glass fiber results in more significant increase in fiber tension,

which requires a larger increase in temperature to offset the shrinkage, a temperature profile for an optimized cure with glass fiber may not be the same as that for the carbon fiber. The trends of these profiles would be similar but the maximum temperature would probably be greater for the cure with glass fiber. This means that a specific polymer requires different cure cycles depending on the reinforcement being used.

3.5 Dynamic Testing Results

The glass transition temperature for specimen cured for 240 minutes were tabulated and listed in Table 2. These values were found using the corresponding temperature to the peak of the tan δ curve from the DMTA results shown in Figure 15. The temperature associated with the tan δ peak is indicated with a dashed line. Note that this method of using the tan δ peak is one of several methods used to estimate the T_g, with others using the temperature associated with the initial change in storage modulus, loss modulus or tan δ curves. Depending on which is method is chosen, some fluctuations may occur in the T_g results. Comparing the specimens T_g to that of the standard cure gives an approximation of the degree of cure for each specimen. Typically as the T_g increases, so

Table 2. T_g results from DMTA for specimen with carbon fiber cured for 240 minutes (manufacturer recommended). The isothermal cures exhibit T_g's lower than the standard cure while the optimized cures are higher.

Cure Cycle	Standard Cure	Isothermal Cure at 98.9°C	Isothermal Cure at 110°C	Isothermal Cure at 121.1°C	CLFS Initiated at 98.9°C	CLFS Initiated at 110°C
Tg (°C)	156	139	150	151	158	165
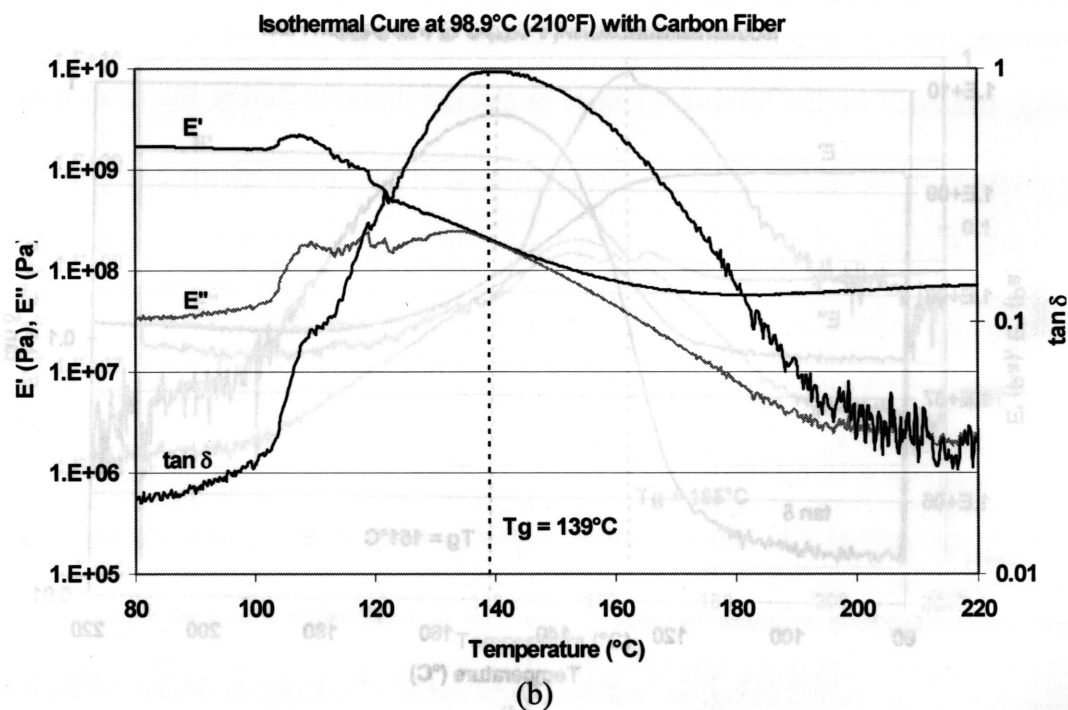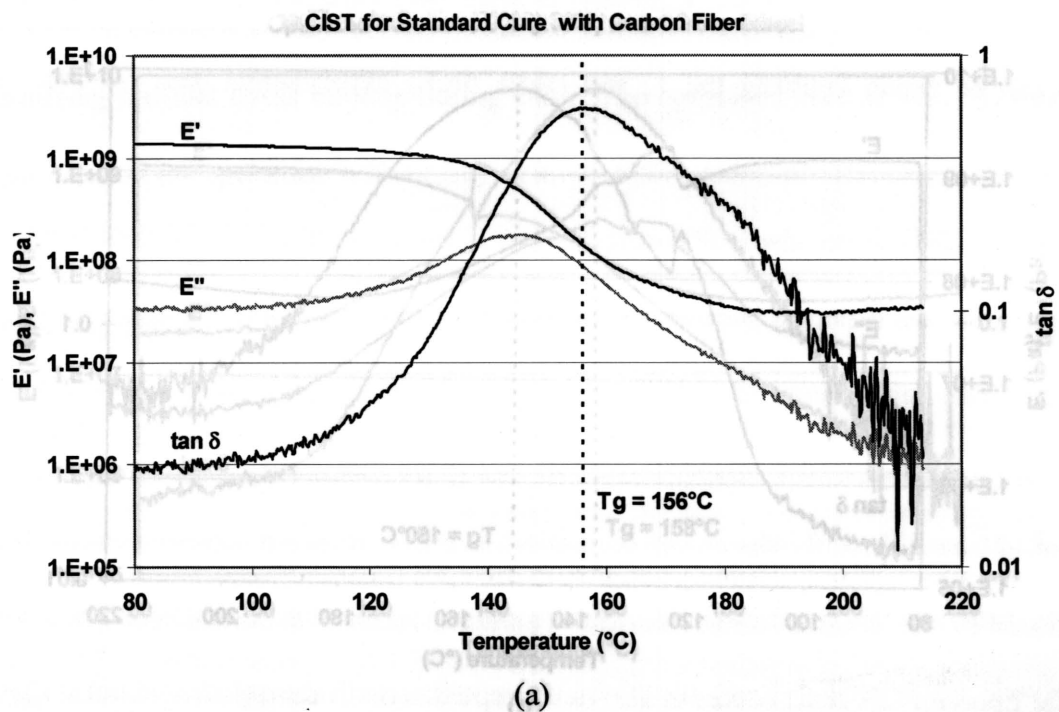
Figure 15. Results from DMTA testing for specimens cured for 240 minutes with Epon/mPDA and carbon fiber using (a) standard cure cycle, (b) isothermal cure at 98.9°C.
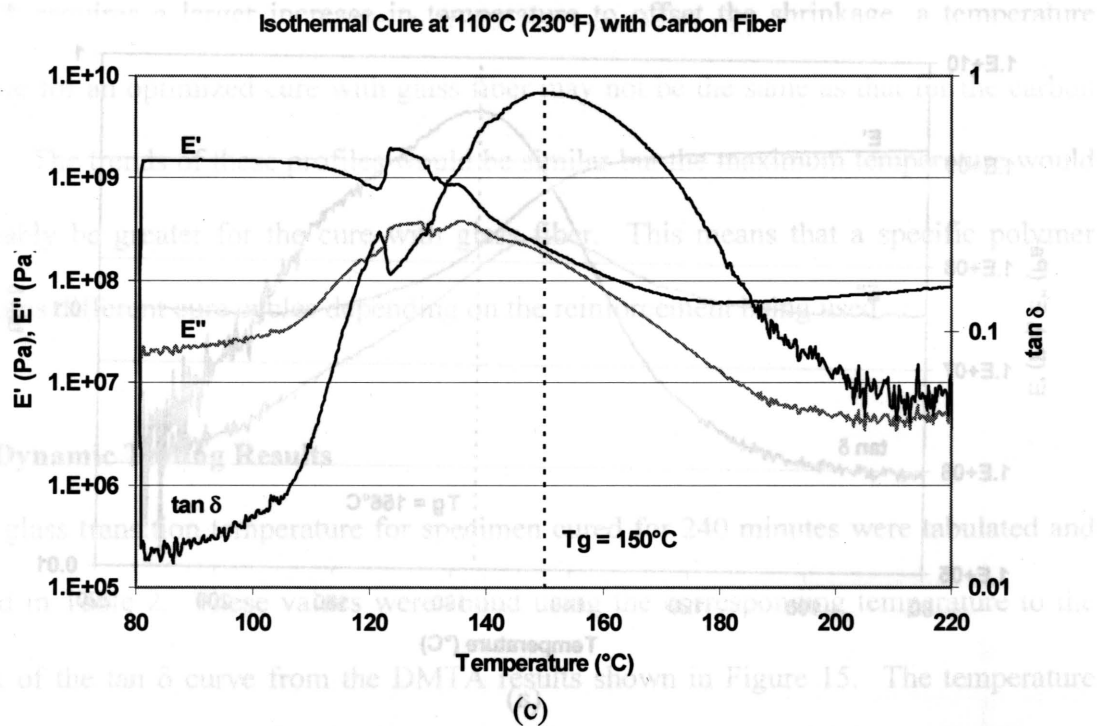
Figure 15. Continued. (c) isothermal cure at 110°C, (d) isothermal cure at 121.1°C.

Optimized Cure at 98.9°C (210°F) with Carbon Fiber

(e)

CLFS at 110°C (230°F) with Carbon Fiber

(f)
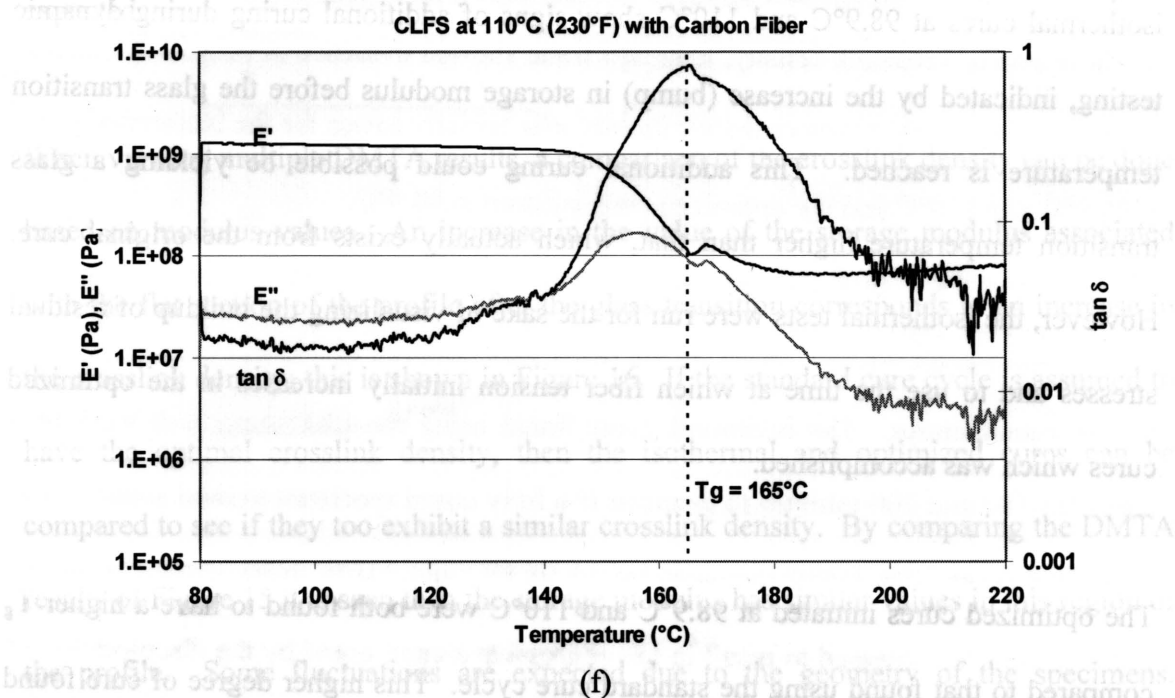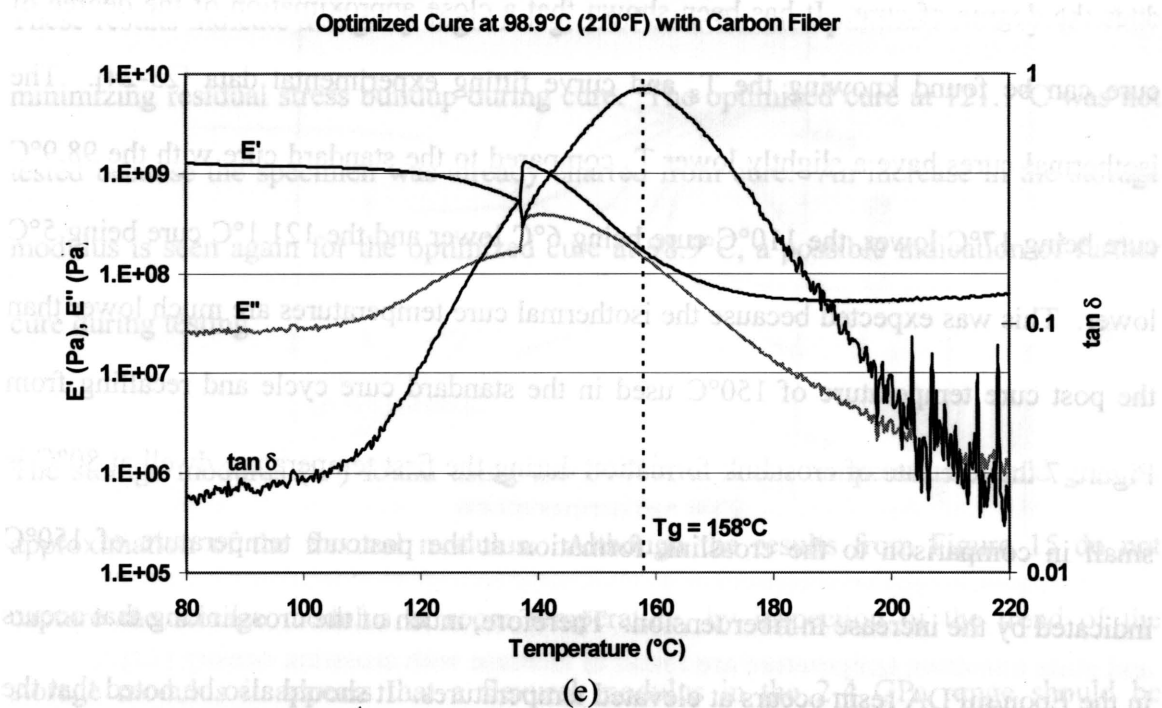
Figure 15. Continued. (e) optimized cure initiated at 98.9°C and (f) optimized cure initiated at 110°C.

41

does the degree of cure. It has been shown that a close approximation of the degree of cure can be found knowing the T_g and curve fitting experimental data [23-24]. The isothermal cures have a slightly lower T_g compared to the standard cure with the 98.9°C cure being 17°C lower, the 110°C cure being 6°C lower and the 121.1°C cure being 5°C lower. This was expected because the isothermal cure temperatures are much lower than the post cure temperature of 150°C used in the standard cure cycle and recalling from Figure 7 that the rate of crosslink formation during the first temperature dwell at 80°C is small in comparison to the crosslink formation at the postcure temperature of 150°C indicated by the increase in fiber tension. Therefore, much of the crosslinking that occurs in the Epon/mPDA resin occurs at elevated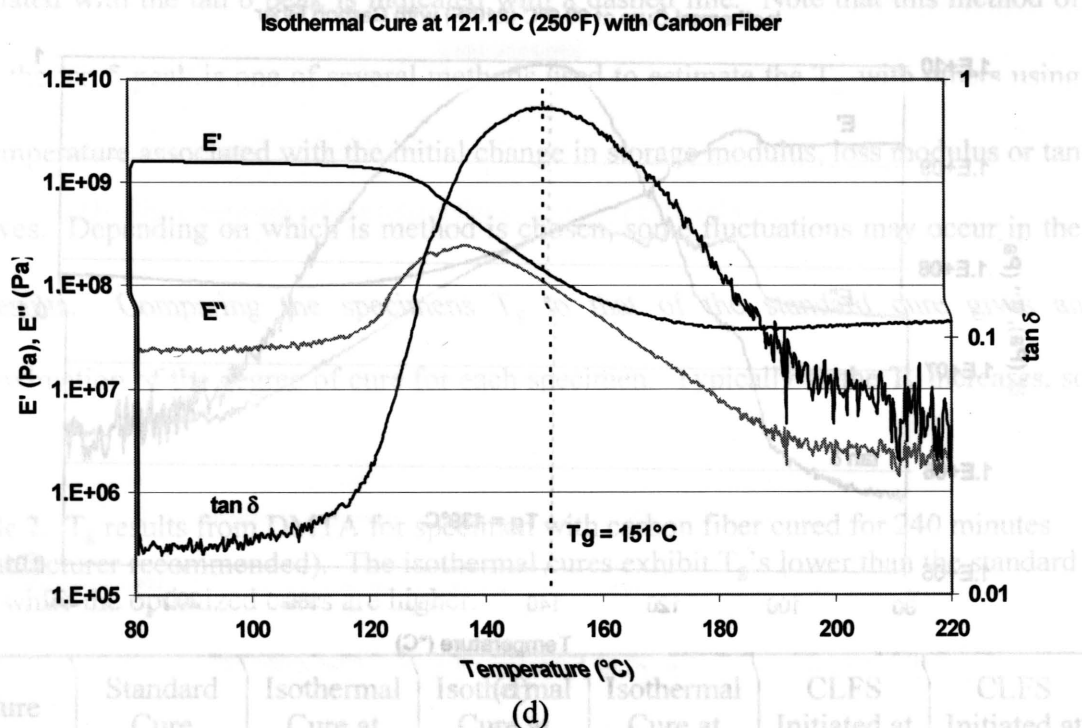 temperatures. It should also be noted that the isothermal cures at 98.9°C and 110°C show signs of additional curing during dynamic testing, indicated by the increase (bump) in storage modulus before the glass transition temperature is reached. This additional curing could possible be yielding a glass transition temperature higher than that, which actually exists from the original cure. However, the isothermal tests were run for the sake of visualizing the buildup of residual stresses and to use the time at which fiber tension initially increases in the optimized cures which was accomplished.

The optimized cures initiated at 98.9°C and 110°C were both found to have a higher T_g compared to that found using the standard cure cycle. This higher degree of cure found using the optimized cure cycle compared to the isothermal cure is most likely due to the elevated temperatures reached in the optimized cure resembling that of the standard cure.

These results indicate a slightly higher degree of cure for the optimized cure cycle while minimizing residual stress buildup during cure. The optimized cure at 121.1°C was not tested because the specimen was already charred from cure. An increase in the storage modulus is seen again for the optimized cure at 98.9°C, a possible indication of further cure during testing.

The storage modulus (E') found using the DMTA at room temperature would give an approximation of the flexural modulus. Although the results from Figure 15 do not capture the storage modulus at room temperature, by inspection of the trend of the storage modulus it appears that a flexural modulus in the 2-4 GPa range should be expected.

When viewing multiple DMTA results, a comparison of the crosslink density can be done based on modulus values. An increase in the value of the storage modulus associated with the flat section of the profile after the glass transition corresponds to an increase in the crosslink density; this is shown in Figure 16. If the standard cure cycle is assumed to have the optimal crosslink density, then the isothermal and optimized cures can be compared to see if they too exhibit a similar crosslink density. By comparing the DMTA results of Figure 15 it is seen than the storage modulus has similar values in this region of the profile. Some fluctuations are expected due to the geometry of the specimens. However, the trends do show similar features and there is no significant difference among the results from different cures. Therefore, the standard, isothermal, and optimized cures
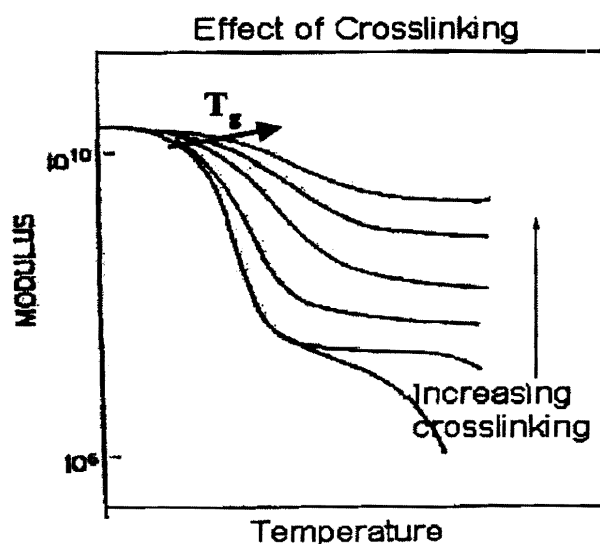
Figure 16. The effects of crosslink density on the DMTA results. Both storage modulus and glass transition temperature are found to increase with crosslink density [22].

all show similar crosslink density, although some showed evidence of additional reaction during testing which means crosslink density was initially lower for the isothermal cures at 98.9°C and 110°C and the optimized cure initiated at 98.9°C.

The above samples were all cured for the same time duration of 240 minutes as specified by the manufacturer. The optimized cures found using the CLFS approach were then cured for 180 and 200 minutes to examine if a fully cured specimen existed sooner. The optimized cures with initial temperatures of 98.9°C and 110°C were chosen since the 121.1°C cure was deemed to result in too aggressive a cure, noted by the discoloration of the specimen. Figure 17 shows the DMTA results for the specimen cured for 180 and 200 minutes. Table 3 shows the glass transition temperatures of the specimen cured for shorter times and Figure 18 compares the T_g results for all specimens.

44
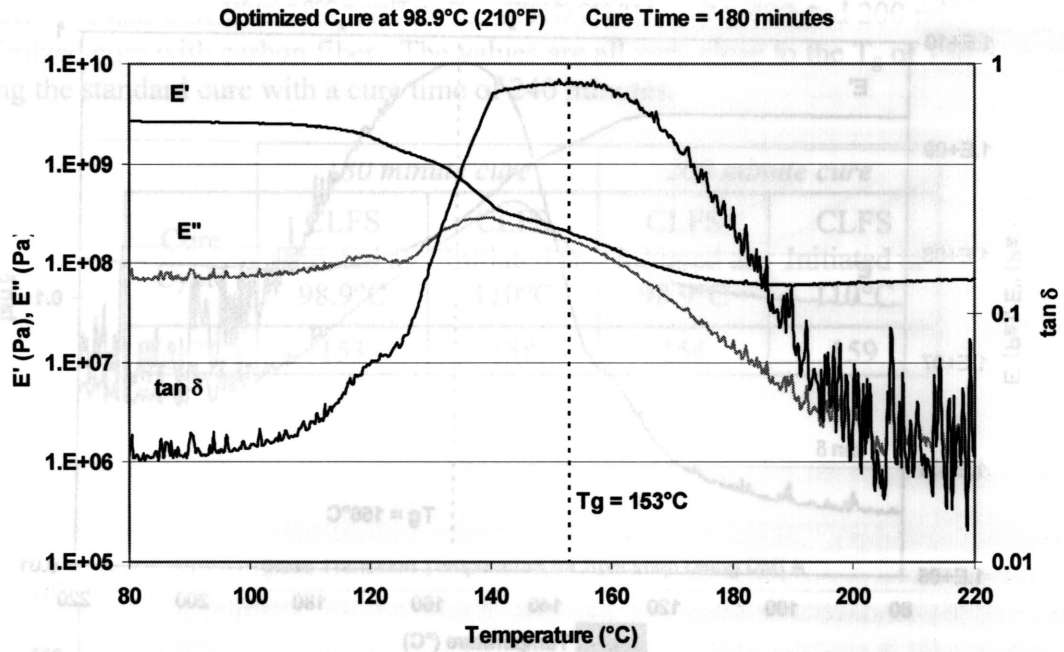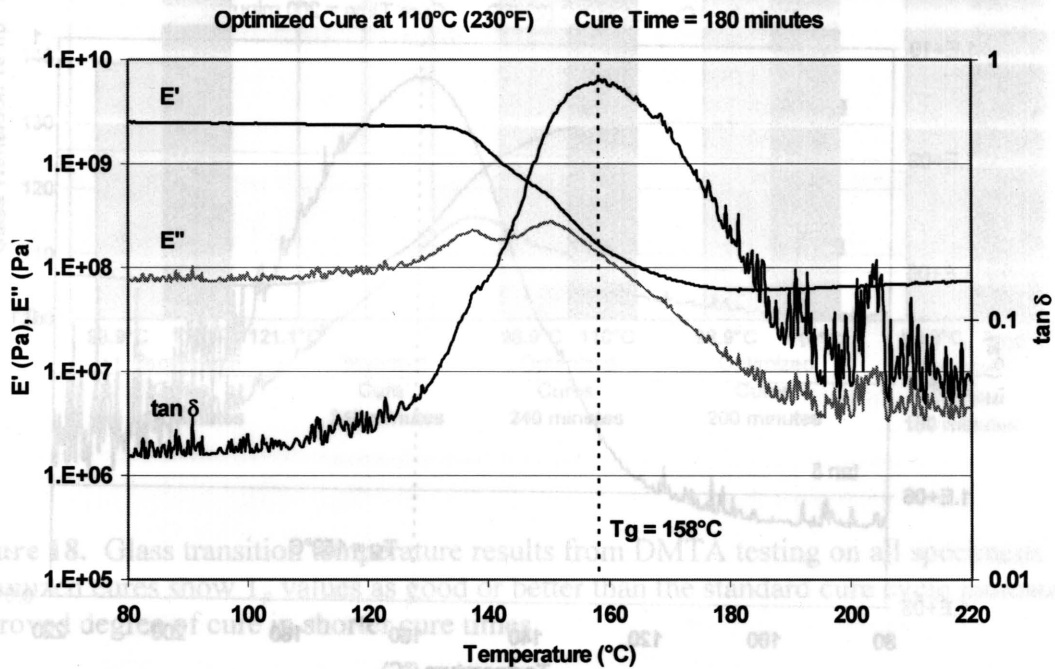
Figure 17. Results from DMTA testing with Epon/mPDA and carbon fiber for (a) optimized cure initiated at 98.9°C and cured for 180 minutes, (b) optimized cure initiated at 110°C and cured for 180 minutes.

Optimized Cure at 98.9°C (210°F)   Cure Time = 200 minutes

E'

E''

tan δ

Tg = 156°C

(c)

Optimized Cure at 110°C (230°F)   Cure Time = 200 minutes

E'

E''

tan δ

Tg = 159°C

(d)
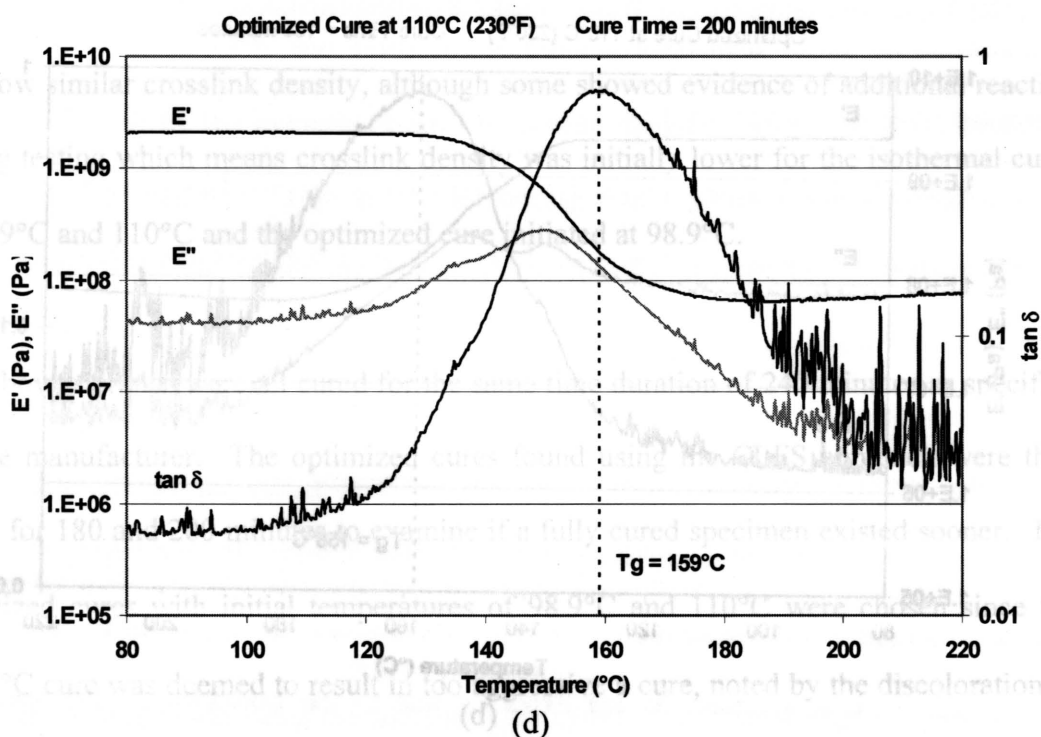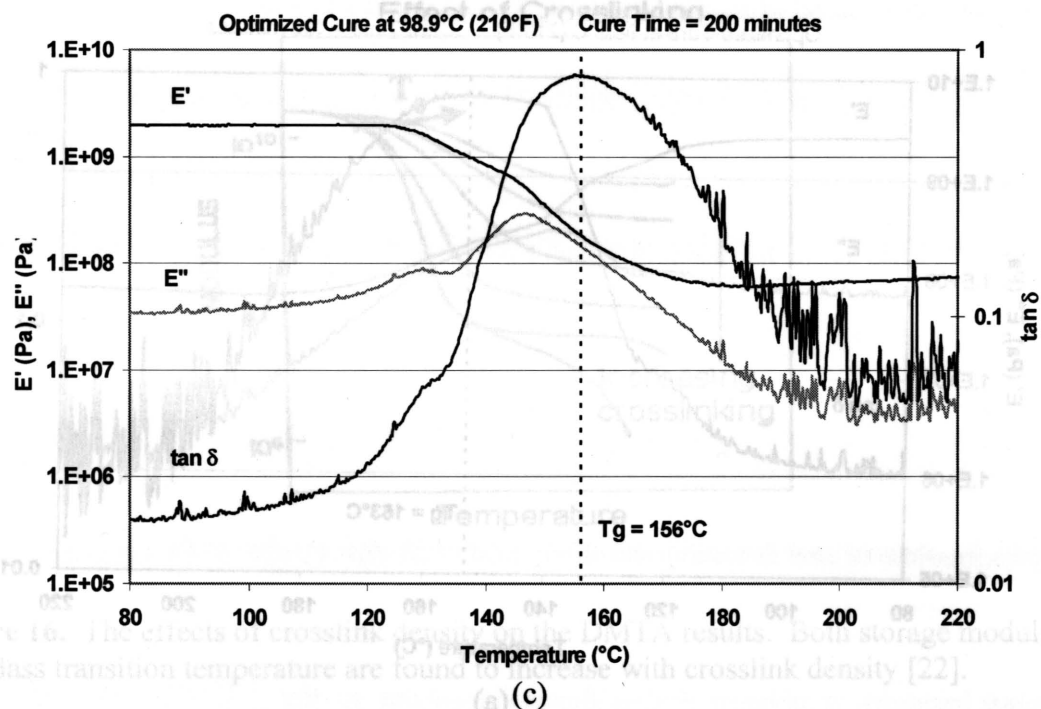
Figure 17. Continued. (c) optimized cure initiated at 98.9°C and cured for 200 minutes and (d) optimized cure initiated at 110°C and cured for 200 minutes.

46

Table 3. Glass transition temperature for specimens cured at 180 and 200 minutes using optimized cure with carbon fiber. The values are all very close to the T_g of 156°C found using the standard cure with a cure time of 240 minutes.

Cure Cycle	180 minute cure		200 minute cure	
	CLFS Initiated at 98.9°C	CLFS Initiated at 110°C	CLFS Initiated at 98.9°C	CLFS Initiated at 110°C
Tg (°C)	153	158	156	159

Glass Transition Temperature for Specimen Using DMTA
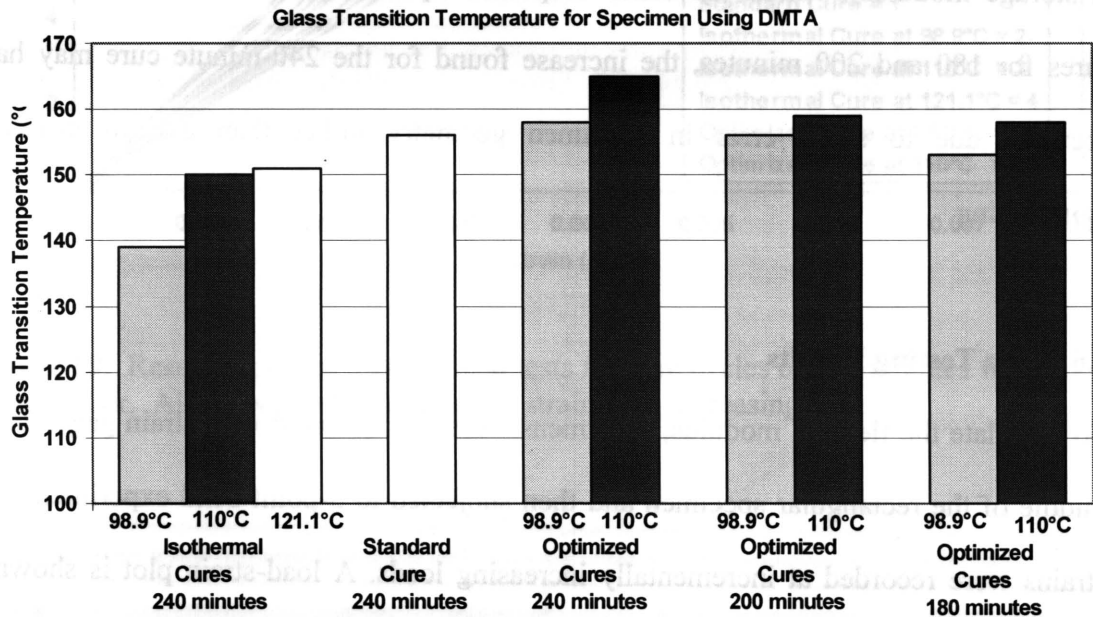
Figure 18. Glass transition temperature results from DMTA testing on all specimens. Optimized cures show T_g values as good or better than the standard cure cycle indicating improved degree of cure in shorter cure times.

The optimized cure initiated at 110°C and cured for 180 minutes shows an improved T_g compared to that found using the standard cure and only required 75% of the total cure time. The optimized cures initiated at 98.9°C and 110°C, and cured for 200 minutes, were found to have T_g's as good or better than the standard cure and did so in 83% of the total cure time recommended by the manufacturer. It is also important to note here that the optimized cures initiated at 98.9°C did not show any additional curing during dynamic testing which was seen before in the specimen cured for 240 minutes (increase in storage modulus). Since the same temperature profile was used for the optimized cures for 180 and 200 minutes, the increase found for the 240-minute cure may have occurred due to slight error in specimen geometry rather than due to increased crosslinking.

3.6 Static Testing Results

To calculate the flexural modulus, specimens were instrumented with strain gages in the middle of the rectangular specimen and then subjected to 3-point bend experiment. The strains were recorded at incrementally increasing loads. A load-strain plot is shown in Figure 19 for all cure cycles cured for the full 240 minutes.

In all cases, the load-strain curves were mostly linear. The stress on a rectangular beam in 3-point bend was calculated using
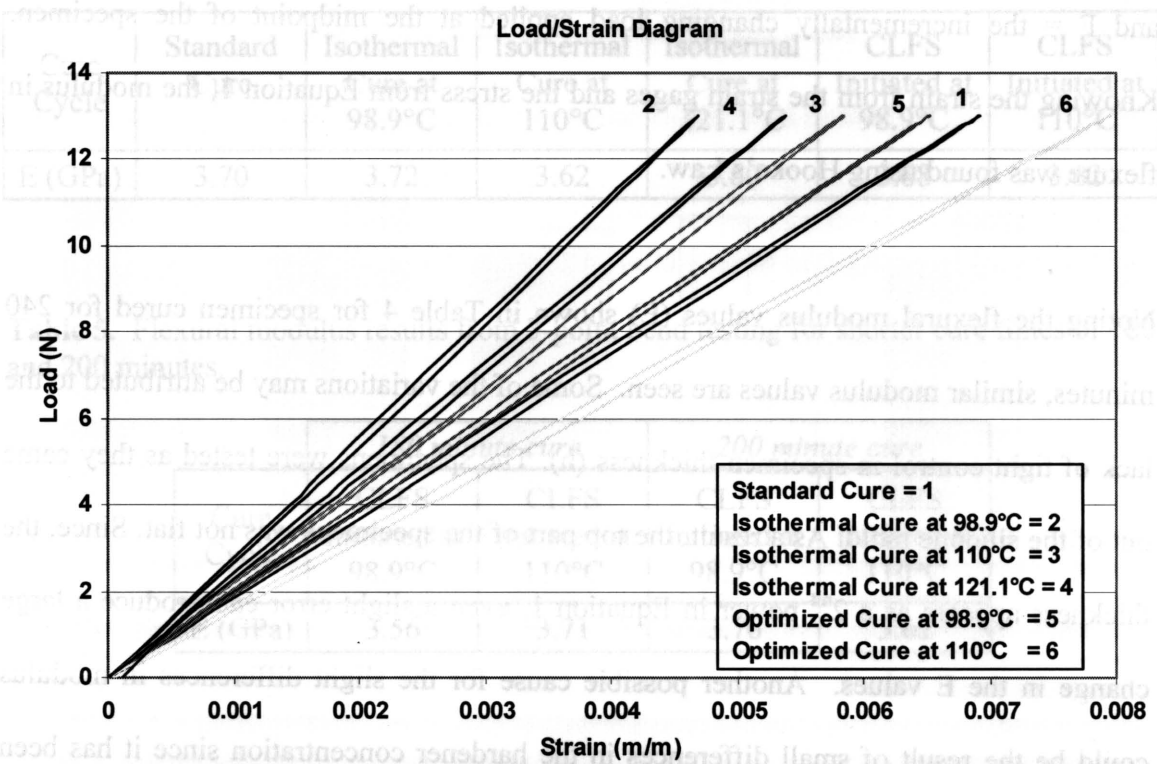
$$\sigma = \frac{3FL}{2bh^2} \qquad [1]$$

Figure 19. Results from the 3-point bend tests for cure cycles of 240 minutes with carbon fiber. All show a linear increase in strain with increasing load.
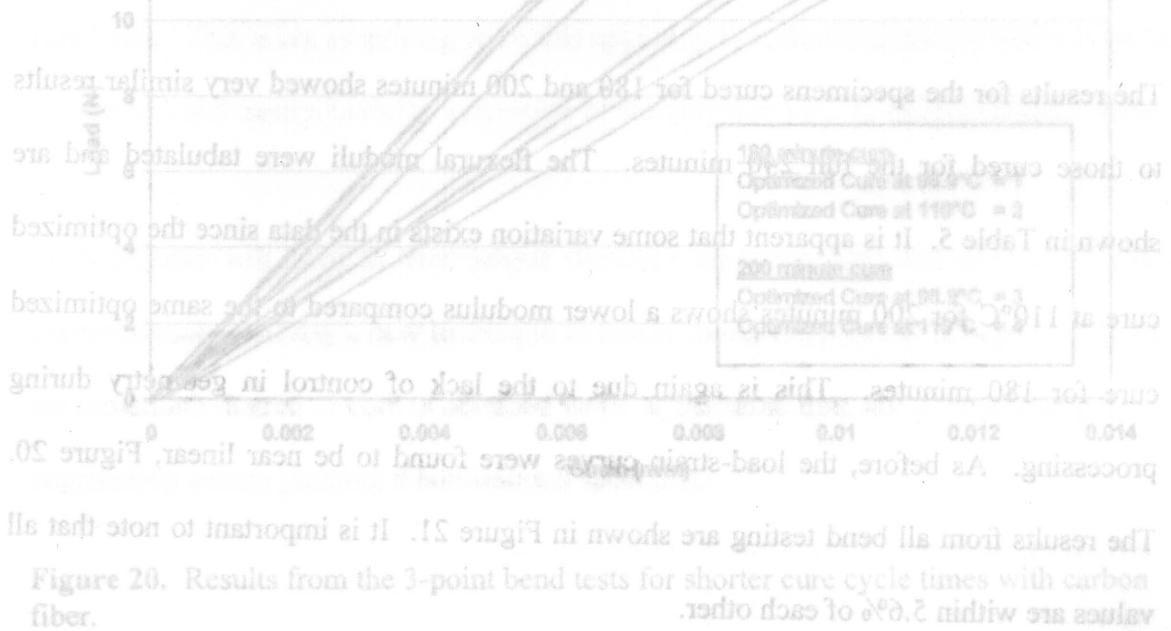
where, L = length between the end supports, b = specimen width, h = specimen thickness, and F = the incrementally changing load applied at the midpoint of the specimen. Knowing the strain from the strain gages and the stress from Equation 1, the modulus in flexure was found using Hooke's Law.

Noting the flexural modulus values (E) shown in Table 4 for specimen cured for 240 minutes, similar modulus values are seen. Some of the variations may be attributed to the lack of tight control in specimen thickness (h). The specimens were tested as they came out of the silicone mold. As a result, the top part of the specimens was not flat. Since, the thickness appears as a 2nd power in Equation 1, even a slight error can produce a large change in the E values. Another possible cause for the slight differences in modulus could be the result of small differences in the hardener concentration since it has been shown that the amount of hardener in a typical epoxy strongly influences the microstructure and consequently the mechanical properties [25].

The results for the specimens cured for 180 and 200 minutes showed very similar results to those cured for the full 240 minutes. The flexural moduli were tabulated and are shown in Table 5. It is apparent that some variation exists in the data since the optimized cure at 110°C for 200 minutes shows a lower modulus compared to the same optimized cure for 180 minutes. This is again due to the lack of control in geometry during processing. As before, the load-strain curves were found to be near linear, Figure 20. The results from all bend testing are shown in Figure 21. It is important to note that all values are within 5.6% of each other.

50

Table 4. Flexural modulus results from static 3-point bend testing

Cure Cycle	Standard Cure	Isothermal Cure at 98.9°C	Isothermal Cure at 110°C	Isothermal Cure at 121.1°C	CLFS Initiated at 98.9°C	CLFS Initiated at 110°C
E (GPa)	3.70	3.72	3.62	3.60	3.68	3.62

Table 5. Flexural modulus results from 3-point bend testing for shorter cure times of 180 and 200 minutes.

Cure Cycle	180 minute cure		200 minute cure	
	CLFS Initiated at 98.9°C	CLFS Initiated at 110°C	CLFS Initiated at 98.9°C	CLFS Initiated at 110°C
E (GPa)	3.56	3.71	3.76	3.62

Load/Strain Diagram

180 minute cure
Optimized Cure at 98.9°C = 1
Optimized Cure at 110°C = 2

200 minute cure
Optimized Cure at 98.9°C = 3
Optimized Cure at 110°C = 4
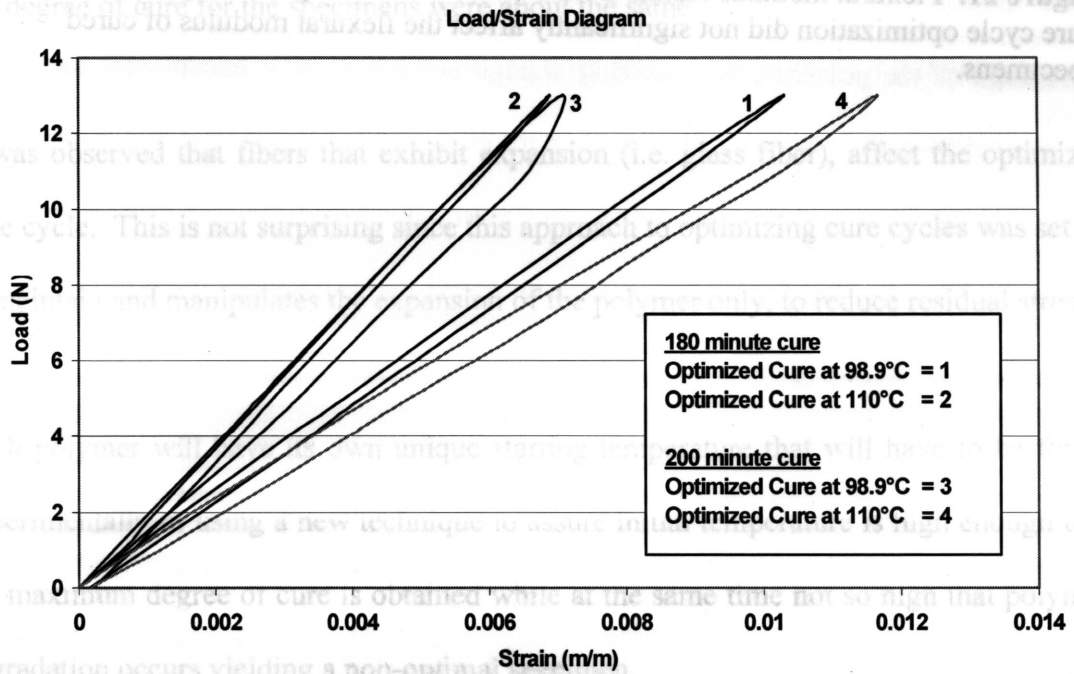
Figure 20. Results from the 3-point bend tests for shorter cure cycle times with carbon fiber.
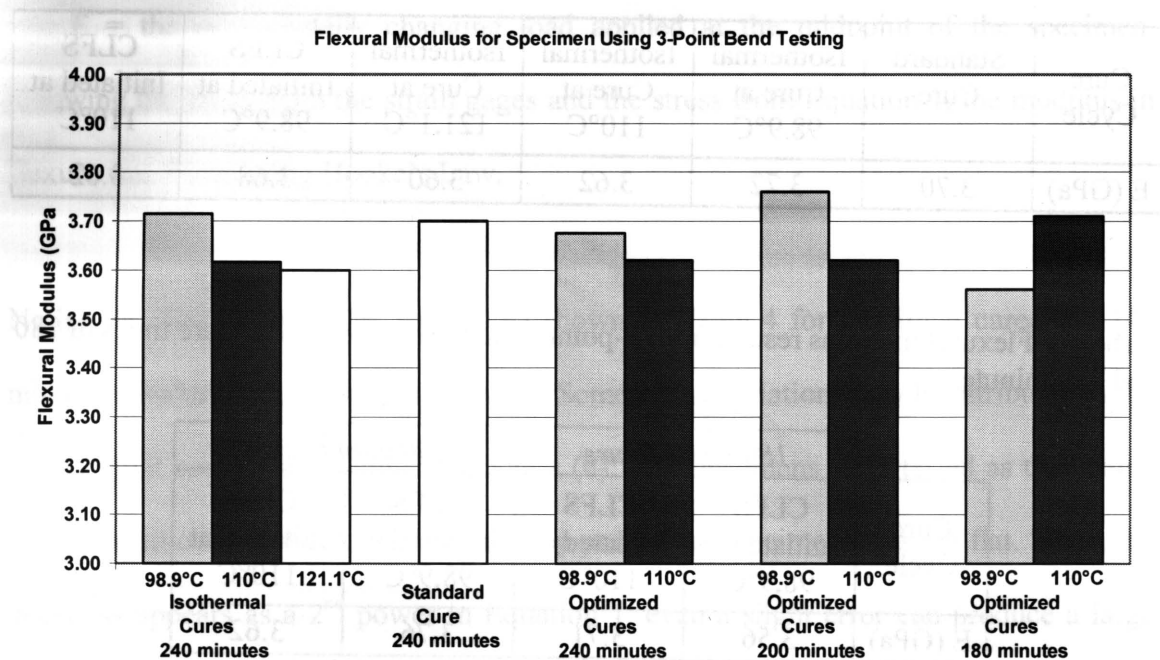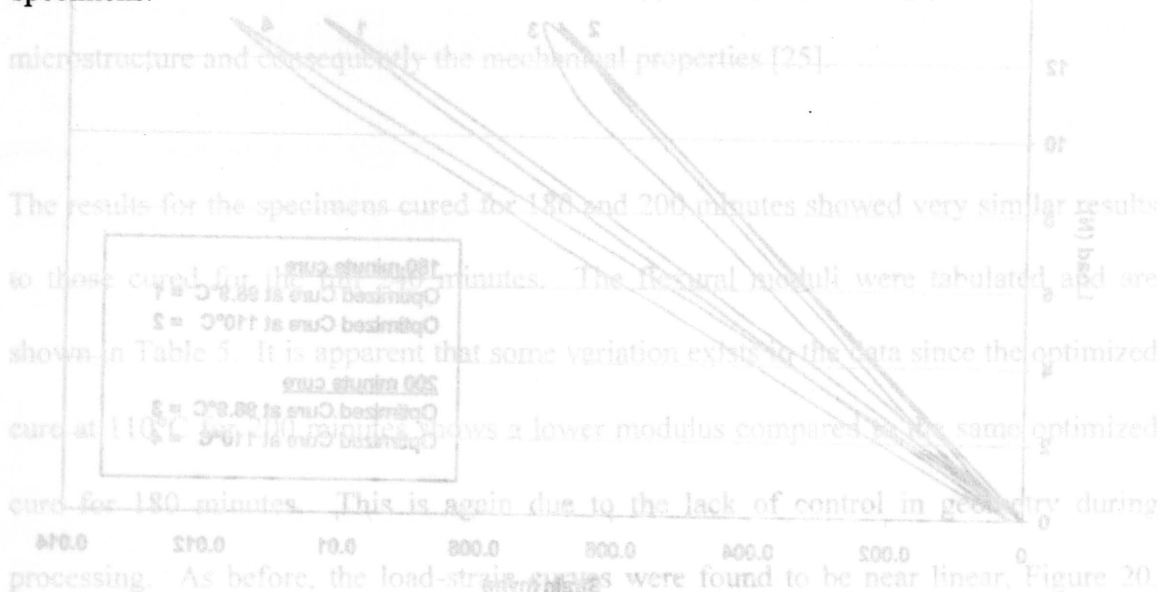
Figure 21. Flexural modulus results from 3-point bend testing on all specimens. The cure cycle optimization did not significantly affect the flexural modulus of cured specimens.

4. Conclusion

A new cure optimization technique has been developed that minimizes residual stresses built up during the cure cycle. The glass transition temperature of the specimens cured using the optimized cure cycle were found to be the same or higher compared to those cured using the standard cure cycle indicating a similar degree of cure for both specimen. In addition, the optimized cure cycle found similar T_g results of the standard cure for cure times of only 75% of the manufacturer recommended cure time.

The flexural modulus of specimens cured using the standard, isothermally cured and using the optimized cure cycles were similar to within 6% of each other as expected since the degree of cure for the specimens were about the same.

It was observed that fibers that exhibit expansion (i.e. glass fiber), affect the optimized cure cycle. This is not surprising since this approach to optimizing cure cycles was set up to maintain and manipulates the expansion of the polymer only, to reduce residual stress.

Each polymer will have its own unique starting temperature that will have to be found experimentally or using a new technique to assure initial temperature is high enough that the maximum degree of cure is obtained while at the same time not so high that polymer degradation occurs yielding a non-optimal specimen.

5. Future Work

The closed loop feedback system (CLFS) is a novel approach to optimizing cure cycles. However, there are a couple of things missing that could greatly improve its performance. The first addition would be to make the program more diverse, that is to say, allow it to perform optimization cures using reinforcements that exhibit expansion such as glass fiber rather than just carbon fiber. This can be done if the expansion of the reinforcement is known as a function of temperature, which for most common reinforcement would be the case. Whether expansion of a fiber is linear or nonlinear, if it is known as a function of temperature it can be used to find the change in fiber length. Knowing the initial length and the tensile modulus of the fiber, the corresponding increase or decrease in fiber tension can be found. As the temperature is increased to offset the chemical shrinkage of the polymer, the resulting change in fiber tension due to heat addition is subtracted from the reference fiber tension resulting in a reference load that changes with time. If the fiber tension falls below the lower bound and the temperature begins to decrease, then the fiber expansion would be added to the transient reference load. The resulting fiber tension profile for a specimen with a thermally expanding fiber would look something like Figure 22. The trend of the temperature profile would not be greatly different from the optimized cure with carbon fiber, but the maximum temperature would be higher for the same initial starting temperature. The idea of the optimized cure approach would still be the same, to cure the polymer around the fiber, so the fiber is essentially unaware that anything is occurring.

54

Possible Optimized Cure for Glass Fiber
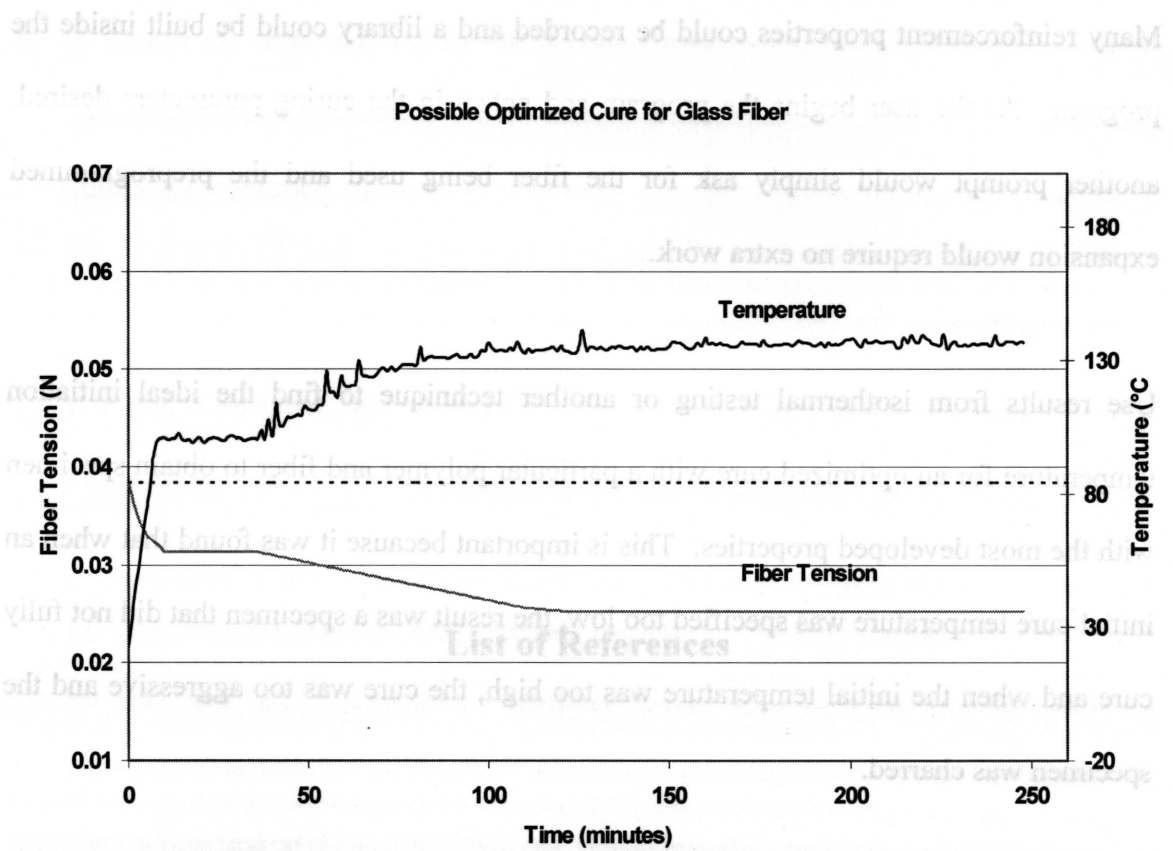
Figure 22. Possible optimized cure cycle for fiber using a modified CLFS program.

Many reinforcement properties could be recorded and a library could be built inside the program. As the user begins the program and enters in the curing parameters desired, another prompt would simply ask for the fiber being used and the preprogrammed expansion would require no extra work.

Use results from isothermal testing or another technique to find the ideal initiation temperature for an optimized cure with a particular polymer and fiber to obtain specimen with the most developed properties. This is important because it was found that when an initial cure temperature was specified too low, the result was a specimen that did not fully cure and when the initial temperature was too high, the cure was too aggressive and the specimen was charred.

List of References

1. R. L. Karkkainen and M. S. Madhukar, "Empirical Modeling of In-Cure Volume Changes of 3501-6 Epoxy," SAMPE, 45th International SAMPE Symposium, 123 (May 2000).

2. J.D. Russell, "Cure Shrinkage of Thermoset Composites," SAMPE Quarterly, 24, (2) 28 (1993).

3. J. Lange, S. Toll and J. Manson, "Residual Stresses Build-up in Thermoset Films Cured Below Their Ultimate Glass Transition Temperatures," Polymer, 38, (4), 809 (1997).

4. A. K. Gopal, S. Adali and V. E. Verijenko, "Optimal Temperature Profiles for Minimum Residual Stress in the Cure Process of Polymer Composites." Composite Structures, 48, (1-3), 99 (2000).

5. O. Sicot, X.L. Gong, A. Cherouat and J. Lu, "Influence of Experimental Parameters on Determination of Residual Stress Using the Incremental Hole-Drilling Method," Composites Science and Technology, 64, (2) 171 (2004).

6. O. Vardar and N. Ersoy, "Measurement of Residual Stresses in Layered Composites by Compliance Method," Journal of Composite Materials, 34, (7) 575 (2000).

7. Y.M. Xing, S. Kishimoto, Y. Tanaka and N. Shinya, "A Novel Method for Determining Interfacial Residual Stress in Fiber Reinforced Composites," Journal of Composite Materials, 38, (2) 137 (2004).

8. D.J. Michaud, A.N. Beris and P.S. Dhurjati, "Thick-Sectioned RTM Composite Manufacturing, Part II. Robust Cure Cycle Optimization and Control," Journal of Composite Materials, 36, (10) 1201 (2002).

9. Q. Zhu, P.H. Geubelle, M. Li and C. L. Tucker III. "Dimensional Accuracy of Thermoset Composites: Simulation of Process-Induced Residual Stresses." Journal of Composite Materials, 35, (24), 2171 (2001).

10. T.A. Bogetti and J.W. Gillespie Jr., "Two-Dimensional Cure Simulation of Thick Thermosetting Composites," Journal of Composite Materials, 25, (3) 239 (1991).

11. V. Pillai, A.N. Beris and P Dhurjati. "Intelligent Curing of Thick Composites Using a Knowledge-Based System." Journal of Composite Materials, 31, (1) 22 (1997).

12. K. M. Nelson, "Cure Kinetics and the Dimensional Control of Composite Structures." 45th International SAMPE Symposium, 156 (May 2000).

13. N. Rai and R. Pitchumani, "Optimal Cure Cycles for the Fabrication of Thermosetting-Matrix Composites." Polymer Composites, 18, (4), 566 (1997).

14. S.R. White and H.T. Hahn, "Process Modeling of Composite Materials: Residual Stress Development During Cure. Part I. Model Formulation," Journal of Composite Materials, 26, (16) 2402 (1992).

15. S.R. White and H.T. Hahn, "Process Modeling of Composite Materials: Residual Stress Development During Cure. Part II. Experimental Validation," Journal of Composite Materials, 26, (16) 2423 (1992).

16. Y.K. Kim, "Process-Induced Residual Stress Analysis by Resin Transfer Molding," Journal of Composite Materials, 38, (11) 959 (2004).

17. R. Y. Kim, B. P. Rice and A. S. Crasto, "Influence of Process Cycle on Residual Stress Development in BMI Composites," 45th International SAMPE Symposium, (May 2000).

18. M. S. Genidy and M. S. Madhukar, "An Investigation of Cure Induced Stresses in Low Cure Temperature Thermoset Polymer Composites," Journal of Reinforced Plastics and Composites, 18, (14), 1304 (1999).

19. M. S. Genidy, M. S. Madhukar and J. D. Russell, "A Feedback System to Obtain an Optimum Cure Cycle for Thermoset Matrix Composites," 42nd International SAMPE Technical Conference, 302 (October 1997).

20. M. S. Genidy, M. S. Madhukar and J. D. Russell, "A New Method to Reduce Cure-Induced Stresses in Thermoset Polymer Composites, Part I: Test Method," Journal of Composite Materials, 34, (22), 1882 (2000).

21. M.S. Genidy, "On the Reduction of Cure-Induced Stresses in Thermoset Polymer Composites," M.S. Thesis, University of Tennessee, TN, 1999.

22. Menard, Kevin P., Dynamic Mechanical Analysis: A Practical Introduction, Boca Raton: CRC Press, 1999.

23. Y. K. Kim and S. R. White, "Stress Relaxation Behavior of 3501-6 Epoxy Resin During Cure," Polymer Engineering Science, 36, (23) 2852 (1996).

24. J. Kim, T.J. Moon and J.R. Howell, "Cure Kinetic Model, Heat of Reaction, and Glass Transition Temperature of AS4/3501-6 Graphite-Epoxy Prepregs," Journal of Composite Materials, 36, (21), 2479 (2002).

25. J. Wolfrum and G.W. Ehrenstein, "Interdependence Between the Curing, Structure, and the Mechanical Properties of Phenolic Resins," Journal of Applied Polymer Science, 74, (13) 3173 (1999).

Vita

Richard Wayne Burgess was born in Saint Charles, Missouri on July 29, 1979. He spent a portion of his early years growing up in Saint Charles and then later moved to Fort Collins, Colorado in the summer of 1986. He obtained his high school diploma from Rocky Mountain High School in 1997. From there, Richard went to Colorado State University in Fort Collins and received a B.S. in mechanical engineering in the spring of 2002. In August of 2003 he began his graduate studies at the University of Tennessee, Knoxville in aerospace engineering working with Dr. Madhu Madhukar as his major professor. The M.S. degree will be granted in May 2005 upon publication of this study. Currently, Richard is seeking a professional position as an engineer.